

DOT/FAA/AR-07/57

Air Traffic Organization
Operations Planning
Office of Aviation Research
and Development
Washington, DC 20591

Flammability Properties of Aircraft Carbon-Fiber Structural Composite

October 2007

Final Report

This document is available to the U.S. public
through the National Technical Information
Service (NTIS), Springfield, Virginia 22161.



U.S. Department of Transportation
Federal Aviation Administration

NOTICE

This document is disseminated under the sponsorship of the U.S. Department of Transportation in the interest of information exchange. The United States Government assumes no liability for the contents or use thereof. The United States Government does not endorse products or manufacturers. Trade or manufacturer's names appear herein solely because they are considered essential to the objective of this report. This document does not constitute FAA certification policy. Consult your local FAA aircraft certification office as to its use.

This report is available at the Federal Aviation Administration William J. Hughes Technical Center's Full-Text Technical Reports page: actlibrary.tc.faa.gov in Adobe Acrobat portable document format (PDF).

1. Report No. DOT/FAA/AR-07/57		2. Government Accession No.		3. Recipient's Catalog No.	
4. Title and Subtitle FLAMMABILITY PROPERTIES OF AIRCRAFT CARBON-FIBER STRUCTURAL COMPOSITE				5. Report Date October 2007	
				6. Performing Organization Code	
7. Author(s) James G. Quintiere*, Richard N. Walters, and Sean Crowley				8. Performing Organization Report No.	
9. Performing Organization Name and Address Federal Aviation Administration William J. Hughes Technical Center Airport & Aircraft Safety Research & Development Division Fire Safety Section Atlantic City International Airport, NJ 08405 *Dept of Fire Protection Engineering University of Maryland OISI Glenn L. Martin Hall (Bldg. 088) College Park, MD 20742				10. Work Unit No. (TRAIS)	
				11. Contract or Grant No.	
12. Sponsoring Agency Name and Address U.S. Department of Transportation Federal Aviation Administration Air Traffic Organization Operations Planning Office of Aviation Research and Development Washington, DC 20591				13. Type of Report and Period Covered Final Report	
				14. Sponsoring Agency Code ANM-115	
15. Supplementary Notes					
16. Abstract This study investigated the flammability of a carbon-fiber composite material for use in aircraft structures. In particular, it considered a composite material manufactured by Toray Composites (America) to Boeing Material Specification 8-276. The objective was to establish a complete set of properties pertaining to the heating and burning characteristics of these materials in fires. Several apparatuses were used, including the cone calorimeter, microscale combustion calorimeter, thermogravimetric analyzer, differential scanning calorimeter, and a flame spread rig to promote spread with preheating by radiation. An attempt was made to measure the thermal conductivity of the composite over a range of temperatures through its decomposition, but the heat losses from the apparatus likely caused an overestimate in the measurement. Data from standard tests were also reported for the Ohio State University calorimeter and the smoke density chamber. The material burns in a manner similar to a charring material, in that the carbon fibers comprise most of its mass. The composite burns primarily from the vaporization of its resin. It can ignite with a pilot flame after preheating at a low heat flux. When it burns, the resin vapor is forced out of the fiber pores, and pressure causes the material to swell to over twice its volume. In most all cases studied, the composite maintained its rigidity, but its structural strength was not examined after degradation. The material appears to maintain homogeneity in swelling. The fibers create an insulating, char-like structure that causes a reduction in the internal heating, and consequently, the burning rate drops in time. As the burning rate drops, extinction can naturally occur due to insufficient heating. As is common of charring materials, external heat flux is required to sustain burning and flame spread. It should be noted that the carbon fiber can also oxidize under high-temperature conditions, and this was observed even at low heat fluxes. Furthermore, the properties in this report pertain primarily to the characteristics of the resin material, as the carbon fibers are essentially inert. The data in this report can be used for modeling and explaining the fire behavior of the composite in fire scenarios associated with aircraft operations.					
17. Key Words Carbon fiber, Composite, Flame spread, Heat release			18. Distribution Statement This document is available to the U.S. public through the National Technical Information Service (NTIS) Springfield, Virginia 22161.		
19. Security Classif. (of this report) Unclassified		20. Security Classif. (of this page) Unclassified		21. No. of Pages 43	
				22. Price	

ACKNOWLEDGEMENTS

J.G. Quintiere is indebted to Gus Sarkos and Dick Hill for their support and motivation for this study of carbon-fiber composite material for aircraft construction. Discussions with Richard Lyon on the approach and interpretation of the data have been rewarding and critical to the full understanding of the composite characteristics. Also, the author is grateful to Dr. Lyon for extending the hospitality of the facilities and resources of his group for this study. His staff, Sean Crowley and Richard Walters, are co-authors of this report, and their contributions are greatly appreciated.

TABLE OF CONTENTS

	Page
EXECUTIVE SUMMARY	ix
1. INTRODUCTION	1
2. EXPERIMENTAL MEASUREMENTS	2
2.1 Thermal Conductivity	3
2.2 Thermodynamic Properties	4
2.3 Kinetics of Degradation	6
2.4 Ignition	8
2.5 Burning	11
2.6 Yields and Morphology of Burning	19
2.7 Yields of Incomplete Combustion Products	25
2.8 Flame Spread	28
3. SUMMARY OF RESULTS	31
4. CONCLUSIONS	33
5. REFERENCES	33

LIST OF FIGURES

Figure		Page
1	Toray Carbon-Fiber Composite: Smooth Face, Edge, and Rough Face, Left to Right	1
2	Conduction Apparatus: Heater Plate in Specimen Sandwich With Edge Insulation	3
3	Composite Thermal Conductivity Versus Temperature	4
4	The DSC Results, Specific Heat, and Heat of Decomposition	5
5	Microscale Combustion Calorimeter Results	5
6	Arrhenius Plot to Determine Kinetic Parameters of Thermal Decomposition	7
7	The TGA Results and Comparison to First-Order Model	7
8	Time to Ignite: Piloted and Auto	8
9	Thermal Response Parameter Values From Ignition Delay Experiments	10
10	Thermally Thick Theory Compared to Data for Piloted Ignition	11
11	Heat Release in OSU Calorimeter	12
12	Heat Release Rate per Unit Area at Fluxes From 25 to 100 kW/m ²	13
13	Average Peak HRR Over Burning Range	15
14	Heat of Combustion Over Range of Burning	15
15	The HRR During the Critical Burning Series With Igniter	16
16	Total Energy Released in Burning	17
17	Burning Rate of Carbon Fibers in Smoldering	17
18	Surface Temperatures of Carbon Fiber Smoldering	18
19	Vertical Burning in the OSU Apparatus	19
20a	After Burning Front and Back, 8.2 kW/m ²	20
20b	After Burning Front and Back, 12.3 kW/m ²	20
20c	After Burning Front and Back, 14.7 kW/m ²	20
20d	After Heating Front and Back, 17.5 kW/m ²	21
20e	After Burning Front and Back, 18.7 kW/m ²	21
20f	After Burning Front and Back, 40.0 kW/m ²	21
20g	After Burning Front and Back, 60.0 kW/m ²	22
20h	After Burning Front and Back, 85 kW/m ²	22
21	Thickness Increase on Burning	23
22	Morphology of Composite After Burning	24
23	Cross Section of the 40 kW/m ² Heated Composite	25
24	Yield of CO for Flaming Conditions	25
25	Yield of Smoke for Flaming Conditions	26
26	The D_s for the Smoke Density Chamber	27
27	Residue Fraction After Flaming	27
28	Flame Spread Apparatus	28
29	Vertical Flame Spread	29
30	Pyrolysis and Flame Tip in Vertical Spread	29
31	Flame Speed Dependence on Heat Flux	30
32	Upward Flame Spread Behavior	31

LIST OF TABLES

Table		Page
1	The Results for FAA 14 CFR 25.853 OSU Calorimeter Test	12
2	Summary of Toray Carbon-Fiber Composite	32

LIST OF SYMBOLS AND ACRONYMS

a_p	Pre-exponential factor
β	Heating rate
CO	Carbon monoxide
CO ₂	Carbon dioxide
c_p	Heat capacity
d	Diameter
ΔT	Temperature difference
Δ_{hc}	Average heat of combustion
D_m	Mass optical density
D_s	Specific optical density
E_a	Activation energy
h_c	Heat of combustion
h_g	Heat of gasification per unit mass
k	Thermal conductivity
L	Heat of gasification
m	Mass
δ	Thickness
P	Porosity
\dot{q}''	Heat flux
R	Gas constant
T	Temperature
t	Time
T_{ig}	Ignition temperature
t_{ig}	Time to ignition
μ	Char (residue) fraction
χ	Combustion efficiency
BMS	Boeing Material Specification
CFR	Code of Federal Regulations
CHF	Critical heat flux
DSC	Differential scanning calorimeter
FAA	Federal Aviation Administration
HRP	Heat release parameter
HRR	Heat release rate
J	Joules
K	Kelvin
OSU	Ohio State University
SDC	Smoke density chamber
TGA	Thermal gravimetric analysis
THR	Total heat release
TRP	Thermal Response Parameter
W	Watts

EXECUTIVE SUMMARY

This study investigated the flammability of a carbon-fiber composite material for use in aircraft structures. In particular, it considered a composite material manufactured by Toray Composites (America) to Boeing Material Specification 8-276. The objective was to establish a complete set of properties pertaining to the heating and burning characteristics of these materials in fires. Several apparatuses were used, including the cone calorimeter, microscale combustion calorimeter, thermogravimetric analyzer, differential scanning calorimeter, and a flame spread rig to promote spread with preheating by radiation. An attempt was made to measure the thermal conductivity of the composite over a range of temperatures through its decomposition, but the heat losses from the apparatus likely caused an overestimate in the measurement. Data from standard tests were also reported for the Ohio State University calorimeter and the smoke density chamber.

The material burns in a manner similar to a charring material, in that the carbon fibers comprise most of its mass. The composite burns primarily from the vaporization of its resin. It can ignite with a pilot flame after preheating at a low heat flux. When it burns, the resin vapor is forced out of the fiber pores, and pressure causes the material to swell to over twice its volume. In most all cases studied, the composite maintained its rigidity, but its structural strength was not examined after degradation. The material appears to maintain homogeneity in swelling. The fibers create an insulating, char-like structure that causes a reduction in the internal heating and consequently the burning rate drops in time. As the burning rate drops, extinction can naturally occur due to insufficient heating. As is common of charring materials, external heat flux is required to sustain burning and flame spread. It should be noted that the carbon fiber can also oxidize under high-temperature conditions, and this was observed even at low heat fluxes. Furthermore, the properties in this report pertain primarily to the characteristics of the resin material, as the carbon fibers are essentially inert.

The data in this report can be used for modeling and explaining the fire behavior of the composite in fire scenarios associated with aircraft operations.

1. INTRODUCTION.

This study was motivated by the need to investigate the fire hazard of carbon-fiber composite material for use in aircraft structures. In particular, it considers the material fabricated to Boeing material specification (BMS) 8-276 by Toray Composites (America) in a quasi-isotropic lay-up $[-45,0,45,90]_2$ s of 16 plies. The material consists of resin and continuous carbon fibers, typically $7\text{ }\mu\text{m}$ in diameter. The thickness of the material is 3.2 mm, and the two faces (smooth and rough) along with the edge view are shown in figure 1.

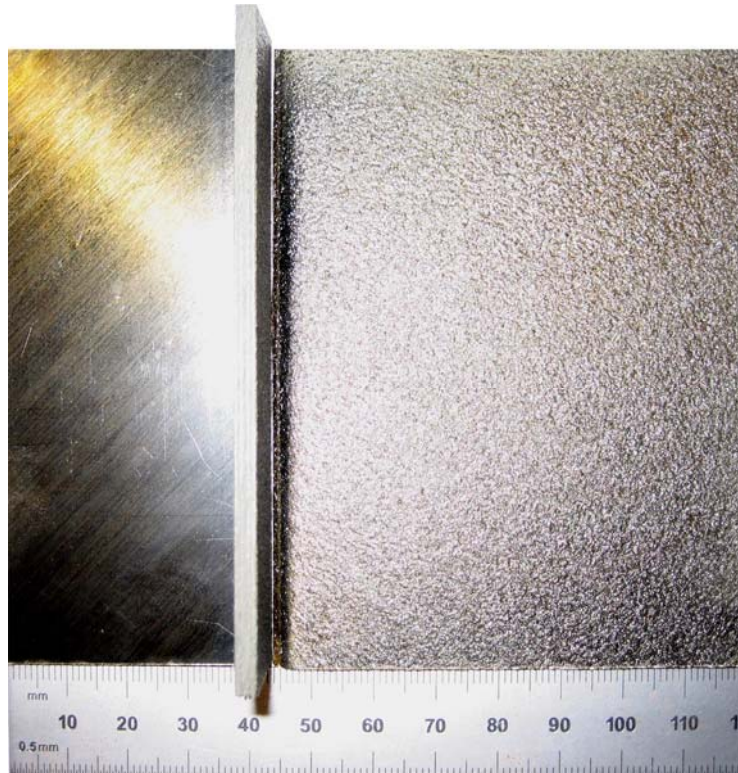


Figure 1. Toray Carbon-Fiber Composite: Smooth Face, Edge, and Rough Face, Left to Right

The density of the composite is $1530 \pm 30\text{ kg/m}^3$. Other physical properties of the composite are listed below:

- Carbon fiber density = 1750 kg/m^3
- Volume fraction of carbon in the composite = 0.60
- Resin density = 1220 kg/m^3
- Char fraction (typical) of resin alone in flaming combustion = 0.25

During heating or combustion, the resin material will vaporize and leave a char residue. The escaping resin vapor must escape through closely spaced carbon fibers. This produces internal pressures in the composite, and the sample will swell. Therefore, the physical properties of the composite will change on heating as the resin vaporizes, because the composite expands in response to the internal pressure. First, the bulk density of the material decreases, then pores form, and finally, the thermal conductivity of the matrix decreases. The strength of the degraded

material is not addressed in this report, but should be a consideration for the effects of fire on its performance. While the vaporization of the resin will allow a flame to form in combustion, the remaining char and carbon can burn as a surface oxidation (smoldering) and even produce a carbon monoxide flame near the oxidizing surface. Typically, surface combustion needs a high temperature to be sustained, which is usually in excess of 500°C.

The use of a carbon composite for aircraft construction can have advantages over aluminum. For example, aluminum will melt at 660°C in large fires. Typically, for a composite material, the degradation temperature to cause burning is 300°-500°C, but it will maintain structural integrity during burning.

Fire produces complex effects in a new material application that are not always anticipated. Since fire is commonly assessed in standard tests, the performance of a new material is not always fully determined. This lack of determination is due to limitations in the tests to indicate pass/fail only, tests designed for traditional materials, and typical scenarios. This report is not intended to address these limitations or scenario considerations, but the data in this report should provide a sufficient basis to make these further analyses. This report will only address the properties of the composite in combustion.

The controlling variable in fire is the heat flux that the material is subjected to. Consequently, the full performance of a material can only be judged by displaying its behavior over an appropriate range of heat flux. This report describes the fire performance over a range of heat flux that encompasses the peak in typical fire situations ($\sim 100 \text{ kW/m}^2$) to the lowest or critical flux that initiates its fire behavior. This report examines the degradation of the material and its behavior in ignition, burning, and flame spread. Special and standard apparatuses have been used to make these measurements. In addition, the thermal, thermodynamic, and chemical degradation kinetics of the material were measured. It should be noted that heat flux in fire would arise due to the flame itself and the thermal feedback of heated surroundings. So, a fire in a confined space will accelerate due to thermal feedback, and oxygen depletion will decelerate the fire.

Therefore, the effect of oxygen is an important factor in combustion, and the use of oxygen supply sources on an aircraft can produce enhanced oxygen. No experiments were conducted to address enhanced oxygen effects, but the theoretical response of this variable is well known, and estimates can be made for its effects.

2. EXPERIMENTAL MEASUREMENTS.

Various apparatuses were used to obtain the data for thermal and combustion effects on the composite. The measurements comprise properties pertaining to thermal, chemical kinetic degradation, and combustion phenomena. Physical properties pertaining to sample decomposition were also measured after combustion. The principal variable varied in the measurements was heat flux, or temperature. The measurements and a description of the apparatus are discussed in the following section.

2.1 THERMAL CONDUCTIVITY.

A flat power source was sandwiched between two identical materials to be measured (see figure 2). The temperature difference (ΔT) across both samples of material was measured. At steady state, half the power (recorded by current and voltage flow) constitutes steady heat conduction through the sample. Consequently, the thermal conductivity (k) can be measured from

$$k = \frac{\dot{q}''\delta}{\Delta T} \quad (1)$$

where δ is the thickness, and \dot{q}'' is the heat flow rate per unit area (heat flux).



Figure 2. Conduction Apparatus: Heater Plate in Specimen Sandwich With Edge Insulation

Measurements were made for the composite by taking the power up in steps, and thereby raising the temperature across the specimen. The results, without accounting for any possible heat losses, are shown in figure 3. A check on the accuracy of the method was made by using 14-mm-thick ThermalCeramics Kaowool® M-board for the sample. Then, the results were compared to ThermalCeramics' published results. The thicker, more insulating M-board caused end heat loss errors of up to 50%. This effect, in the denser, thinner composite suggested heat loss errors could cause a reduction in the results of figure 3 of about 20%. A more accurate, standard test measurement method is recommended to determine the conductivity of the composite. This should be done over the temperature range relevant to burning, as indicated in figure 3.

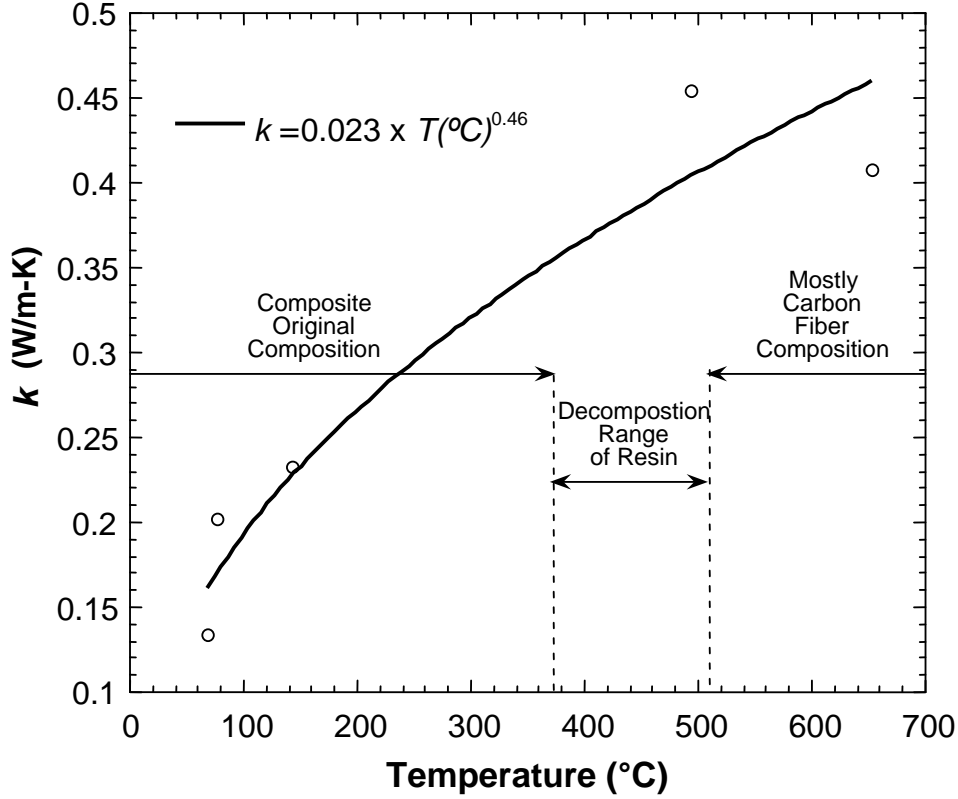


Figure 3. Composite Thermal Conductivity Versus Temperature

2.2 THERMODYNAMIC PROPERTIES.

Specific heat and heat of decomposition were measured by differential scanning calorimetry (DSC) [1]. Appropriate calibrations were done to account for the baseline empty cup, and the heat losses from the heated cup to the surroundings. The sample was taken through decomposition, and then the residue (primarily carbon) was run separately to determine its specific heat. Three repeated runs were averaged for a final value. The results as a function of temperature are shown in figure 4, where J = Joules and K = temperature in Kelvin.

The microscale combustion calorimeter was also used to establish the complete heat of combustion of the volatiles [2]. It measures the energy of complete combustion per unit mass of sample degraded as a function of the sample temperature. These results are shown in figure 5. The heat of complete combustion of the volatiles is determined as

$$\Delta h_{c,complete} = \frac{1}{\beta(1-\mu)} \int_0^\infty \left(\frac{\dot{q}''}{m_i} \right) dT. \quad (2)$$

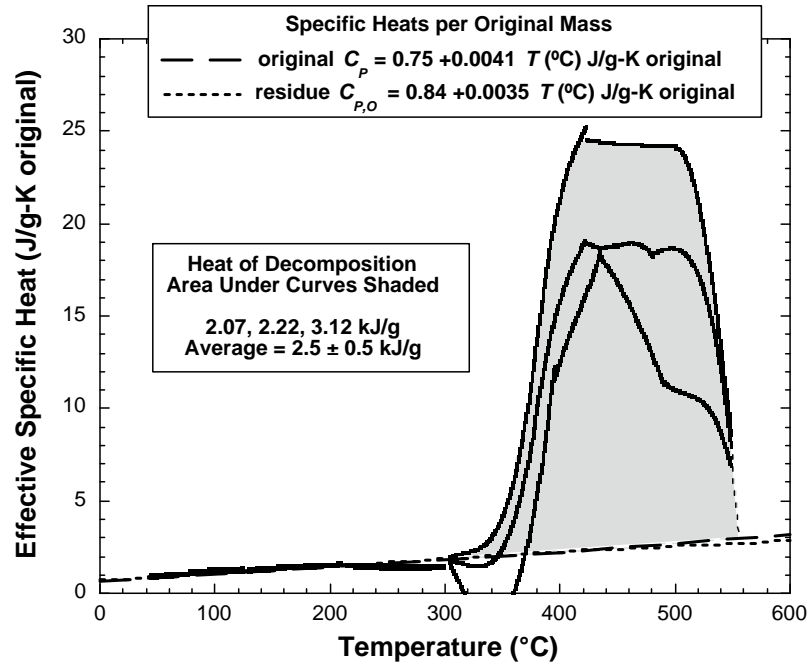


Figure 4. The DSC Results, Specific Heat, and Heat of Decomposition (per Unit Mass of Original Sample)

The heating rate, β , is 1 K/s, and the residue (char) fraction, μ , is 0.74. Performing the integration yields $\Delta h_{c,complete} = 26.5$ kJ/g volatiles.

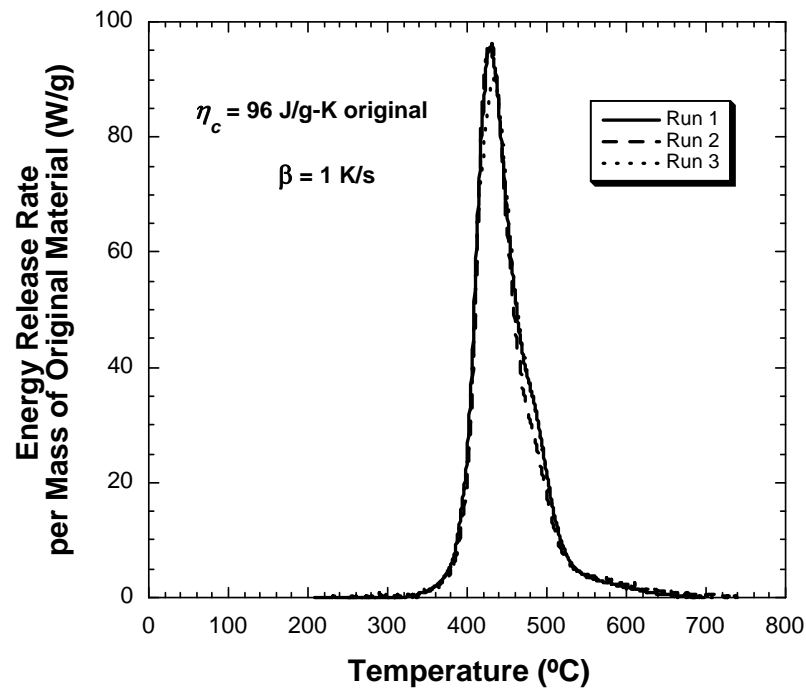


Figure 5. Microscale Combustion Calorimeter Results

2.3 KINETICS OF DEGRADATION.

Standard thermal gravimetric analysis (TGA) was used to establish the degradation and mass loss behavior of the composite in nitrogen. Several runs were made at different heating rates to obtain sufficient data to determine kinetic degradation parameters. A one-step, first-order decomposition model was assumed having activation energy (E_a) and the pre-exponential factor (a_p) for the composite. The char fraction (μ) was also measured. The governing equation for the model is [3]

$$\frac{d\alpha}{dt} = \frac{(1-\alpha)}{(1-\mu)} k(T) \quad (3)$$

where

$$\alpha = \frac{m - m_i}{m_f - m_i} = \frac{\frac{m}{m_i} - 1}{\mu - 1}$$

and m is the mass (i -initial, f -final), and $k = a_p e^{-E_a/RT}$ is the Arrhenius rate. Based on equation 3, the activation energy and pre-exponential constant were determined for four TGA runs of 1°, 3°, 10°, and 30°C/minute at α mass loss rate corresponding to the peak decomposition rate. The result is shown in figure 6, and the kinetic parameters follow as

$$\begin{aligned} E_a &= 182 \text{ kJ/mol} \\ a_p &= 9.67 \times 10^{10} \text{ s}^{-1} \end{aligned}$$

with the residue fraction as $\mu = 0.74$. This fraction in the TGA consists of the carbon fibers and char from the resin.

An exact solution for a small homogeneous sample heated in a TGA at the heating rate β (K/s) is given as [3]

$$\frac{m}{m_i} = \mu - \exp \left[-\frac{a_p}{(1-\mu)\beta} \int_{T_\infty}^T \exp \left(-\frac{E_a}{RT} \right) dt \right] (\mu - 1). \quad (4)$$

The results of the model satisfactorily reproduce the TGA data, as shown in figure 7, except for the end of the process. The model should be suitable for predicting the composite degradation in general, and can be used for fire-modeling analyses. It should be noted that the results of this report could be used in various analytical strategies. The composite can be fully modeled, or aspects of the results can be used to assess specific phenomena. For example, the onset of degradation in the TGA is approximately 300°C, but temperatures in subsequent degradation could reach 400°-500°C at the higher heating rate in a fire (see figure 5).

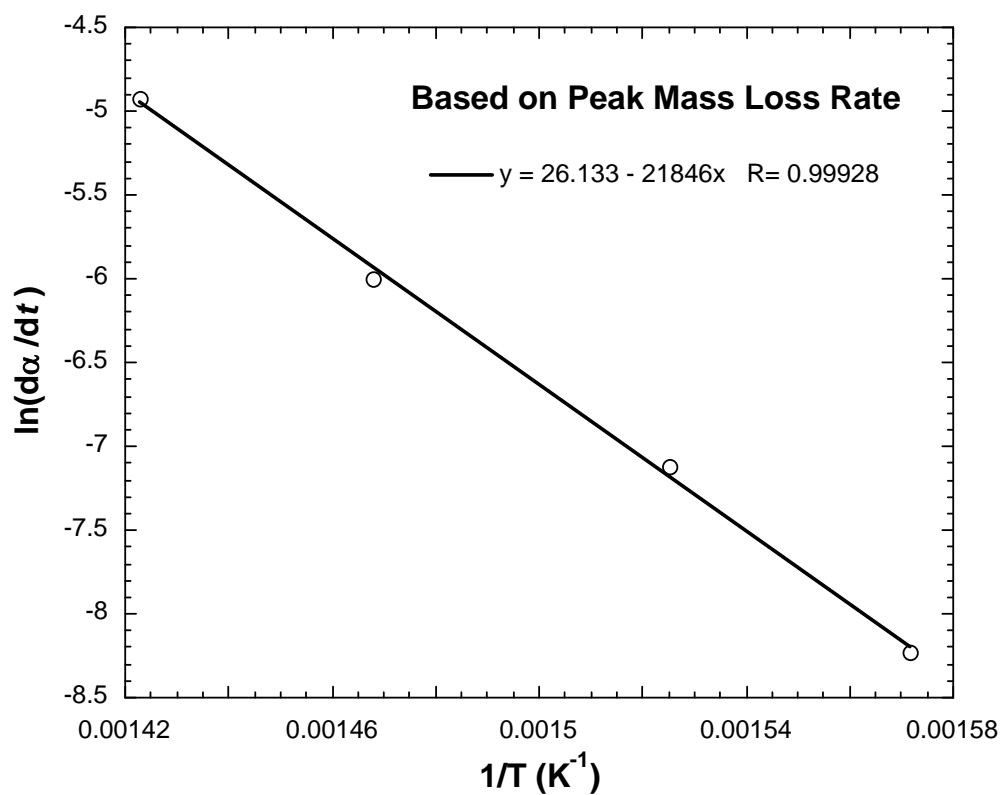


Figure 6. Arrhenius Plot to Determine Kinetic Parameters of Thermal Decomposition

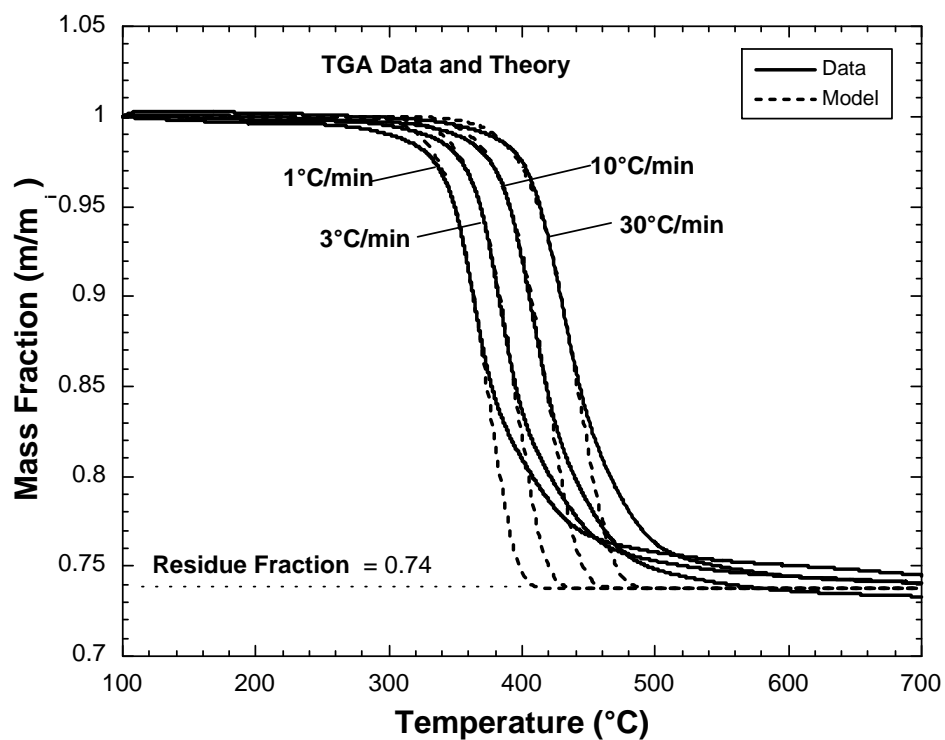


Figure 7. The TGA Results and Comparison to First-Order Model

2.4 IGNITION.

The cone calorimeter was used to conduct ignition and burning experiments over a wide range of heat fluxes. Both piloted and auto-ignition was considered for a horizontal sample. Based on convective heat loss considerations, there is minimal difference between horizontal and vertical ignition under natural convection conditions. In general, ignition time will increase with the velocity of a convective flow. Also, the effect of oxygen in the atmosphere will have minimal effect on ignition, because the degradation temperature of the material where vapor is evolved is most important. The lower flammability limit then controls the onset of piloted ignition, and a sufficient temperature near stoichiometric concentration is needed for auto-ignition. An increase in oxygen concentration has the tendency to reduce the time to ignition (t_{ig}), but the principle time controlling factor is heating the solid to the degradation temperature by conduction.

From TGA/DSC, the onset of vaporization of the composite is about 300°C. After this is attained, both piloted and auto-ignition can occur. They occur at correspondingly higher temperatures, but the piloted ignition temperature (T_{ig}) is typically only slightly higher than the decomposition temperature, because the mass loss rate is very low for piloted ignition. The heat release rate at piloted ignition in air is about 20 kW/m² and about 50 kW/m² to sustain burning [4 and 5].

The time to ignite is summarized in figure 8. It shows that the critical heat fluxes below which ignition cannot occur (in natural convection with radiant heating in air) is 17.5 kW/m² for piloted ignition and about 31.5 kW/m² for auto-ignition. No significant differences were noticed in ignition and burning for heating from either the smooth or rough side of the composite. So, in subsequent tests, only the rough side was examined.

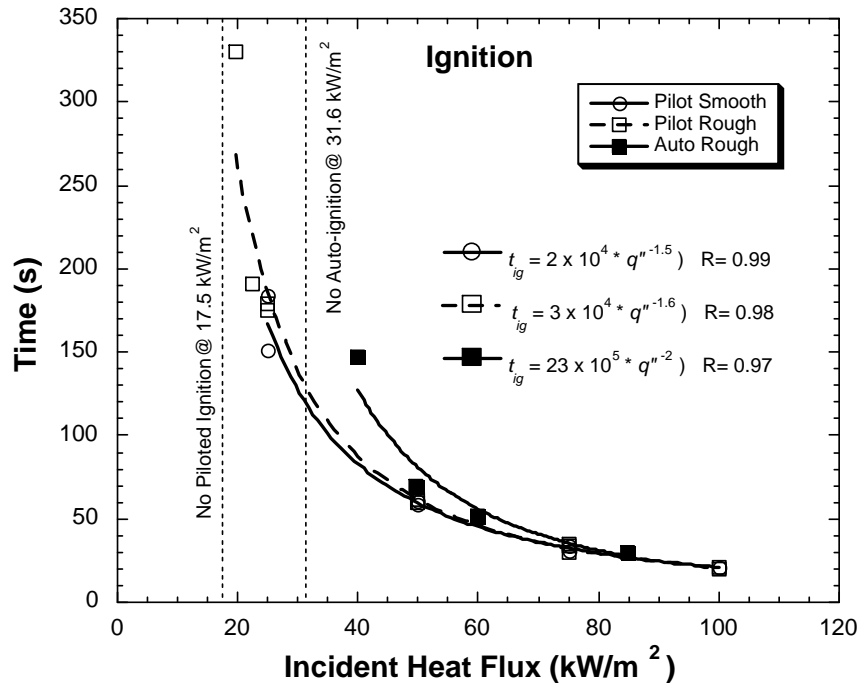


Figure 8. Time to Ignite: Piloted and Auto

Ignition theory based on pure conduction indicates that the time for ignition should behave as heat flux to the -2 power for a thermally thick solid and -1 power for thermally thin. As thermally thick depends on the heat flux, if the physical thickness is greater than the thermal penetration depth as

$$\delta \geq \delta_{ig} = \frac{2k(T_{ig} - T_{\infty})}{\dot{q}_i''}, \quad (5)$$

then the material acts as thermally thick in ignition [3]. For a pilot ignition temperature of 300°C and a thermal conductivity of 0.25 W/m-K, thermally thick results apply for a heat flux greater than 43 kW/m². Hence, one sees that the behavior for auto-ignition appears thermally thick, but not so for piloted ignition at lower heat fluxes.

An important parameter for ignition is the Thermal Response Parameter (TRP). It is defined as

$$TRP = \left(\frac{\pi}{4} k \rho c \right)^{1/2} (T_{ig} - T_0). \quad (6)$$

Several ignition theories for a thermally thick material use TRP to predict the time to ignite. The simplest theory derives from linear conduction theory in the limit of high-incident radiant heat flux, as

$$t_{ig} = \left(\frac{TRP}{\dot{q}_i''} \right)^2. \quad (7)$$

The result may be adjusted to account for the critical flux limit at relatively low heat flux, as

$$t_{ig} = \left(\frac{TRP}{\dot{q}_i'' - \dot{q}_{crit}''} \right)^2. \quad (8)$$

Spearpoint and Quintiere [6] obtained an approximate solution for the corresponding nonlinear effects of re-radiation, as

$$t_{ig} = \left[\frac{\left(\frac{16}{3\pi} \right)}{(2 - \beta_{ig})(1 - \beta_{ig})} \right] \left(\frac{TRP}{\dot{q}_i''} \right)^2, \quad (9)$$

where $\beta_{ig} \equiv \frac{\sigma(T_{ig}^4 - T_0^4) + h_c(T_{ig} - T_0)}{\dot{q}_i''} = \frac{\dot{q}_{crit}''}{\dot{q}_i''}$. The TRP for the composite is found from the slope of $t_{ig}^{-1/2} \propto \dot{q}_i''$, as plotted in figure 9.

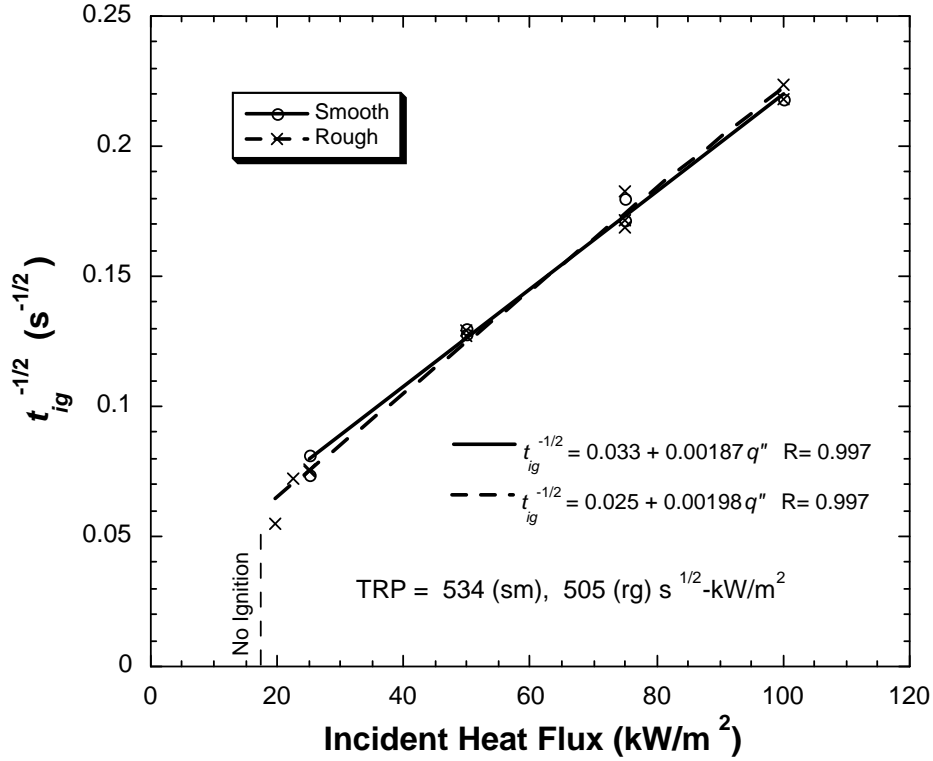


Figure 9. Thermal Response Parameter Values From Ignition Delay Experiments

It is interesting to use the theories of ignition listed above to see how well they reproduce the data. Figure 10 was plotted using average values of $\text{TRP} = 525 \text{ (kW/m}^2\text{)-s}^{1/2}$ and $\dot{q}_{crit}'' = 18 \text{ kW/m}^2$. The theory describes the data only at high heat fluxes, where the sample is thermally thick. While the properties TRP and \dot{q}_{crit}'' found for ignition of the composite are valid, a theory for the prediction of ignition must account for the thin character of the sample at low heat flux.

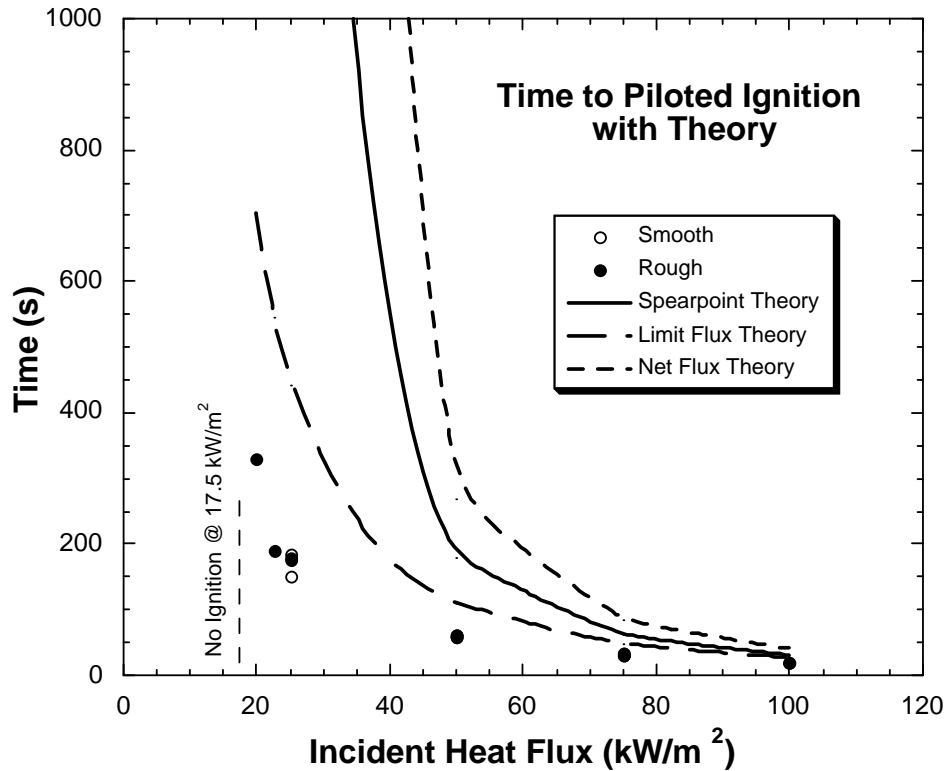


Figure 10. Thermally Thick Theory Compared to Data for Piloted Ignition

2.5 BURNING

The Ohio State University (OSU) fire calorimeter tests were performed according to Title 14 Code of Federal Regulations (CFR) 25.853 a-1 [7], the Federal Aviation Administration (FAA) flammability test method for large surface area materials for aircraft cabin interiors. Tests were performed on 15- by 15-cm (6- by 6-inch) samples with and without the foil backing, and with rough and smooth sides facing outward. Flammability was similar for all samples tested in the different configurations. An average of all the tests is shown in figure 11. Samples ignited 40 to 50 seconds into the test. Large flame jets protruded from the sample surface at 70 to 80 seconds into the test. Initially, it was thought that this occurred because the sample was backed with aluminum foil and the trapped gases had nowhere to go except out the front. Later, tests were performed without the foil backing, and the same sample jetting was observed with additional flames coming from the rear of the sample holder. The values derived from the test were consistent regardless of the sample orientation and the backing foil. Average results for 14 CFR 25.853 are shown in table 1. Samples had a peak heat release rate (HRR) of 104 kW/m^2 at 162 seconds and a 2-minute total heat release (THR) of $73 \text{ kW/m}^2\text{-min}$. The pass/fail criteria of 14 CFR 25.853 a-1 was established for large surface area interior components of passenger aircraft. Samples tested were 16-ply composites to be used for exterior and structural components of the aircraft.

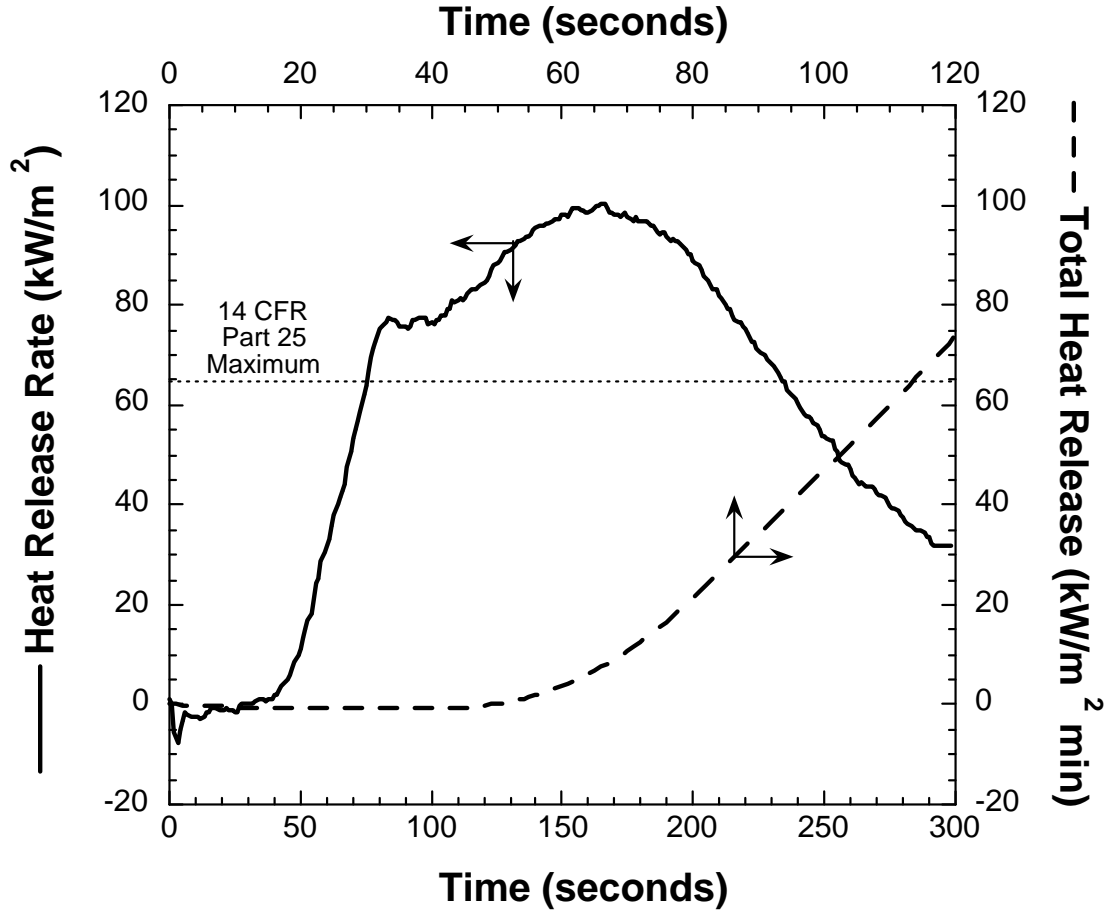


Figure 11. Heat Release in OSU Calorimeter (Average of six tests)

Table 1. The Results for FAA 14 CFR 25.853 OSU Calorimeter Test

	OSU Calorimeter		Smoke Chamber
	Peak HRR (kW/m ²)	2-min THR (kW/m ² -min)	⁴ D _m (--)
Average n=6	104	73	63
FAA Regulation	65	65	200

Cone calorimeter tests were run at incident radiant heat fluxes of 25, 50, 75, and 100 kW/m² according to a standard method [8]. These were done in replicates of at least two for both the smooth and rough side of the composite facing the heat flux in a horizontal orientation. Additional cone tests were performed to determine the minimum heat flux to sustain burning. Following radiant exposure for about 100 s at heat fluxes below the minimum flux for piloted ignition, the sample was forced to ignition by a premixed Bunsen burner flame. As the air for the Bunsen burner was part of the flow stream into the cone system, its oxygen consumption could be used to estimate the contribution from the burner. The subsequent difference from the total energy release rate would be the contribution of the material. In this way, the energy

release rate of the material was determined below the minimum heat flux for ignition. The minimum heat flux for burning could be then established.

Figure 12 shows the results of the standard cone data for fire energy flux (HRR, or heat release rate per unit area). As the heat flux increased over 25 kW/m^2 , the sample responds more as a thermally thick sample [3] producing two peaks in the HRR. The first peak occurs due to the composite seeking to achieve the steady state for the resin binder. As the resin depletes from the surface and into the depth of the material, the carbon fibers form a matrix of insulation. This insulation blocks heat and reduces the HRR. The second peak occurs as the thermal heating wave reaches the back of the composite, and the insulation of the lower density backing board of the cone holder now blocks more heat from being lost. Hence, more heat goes into the sample, and HRR increases until the resin is depleted. This completes the main flaming phase of the composite. However, the carbon and resin char are now capable of oxidizing, and smoldering can ensue with the possibility of a carbon monoxide (CO) flame near the surface.

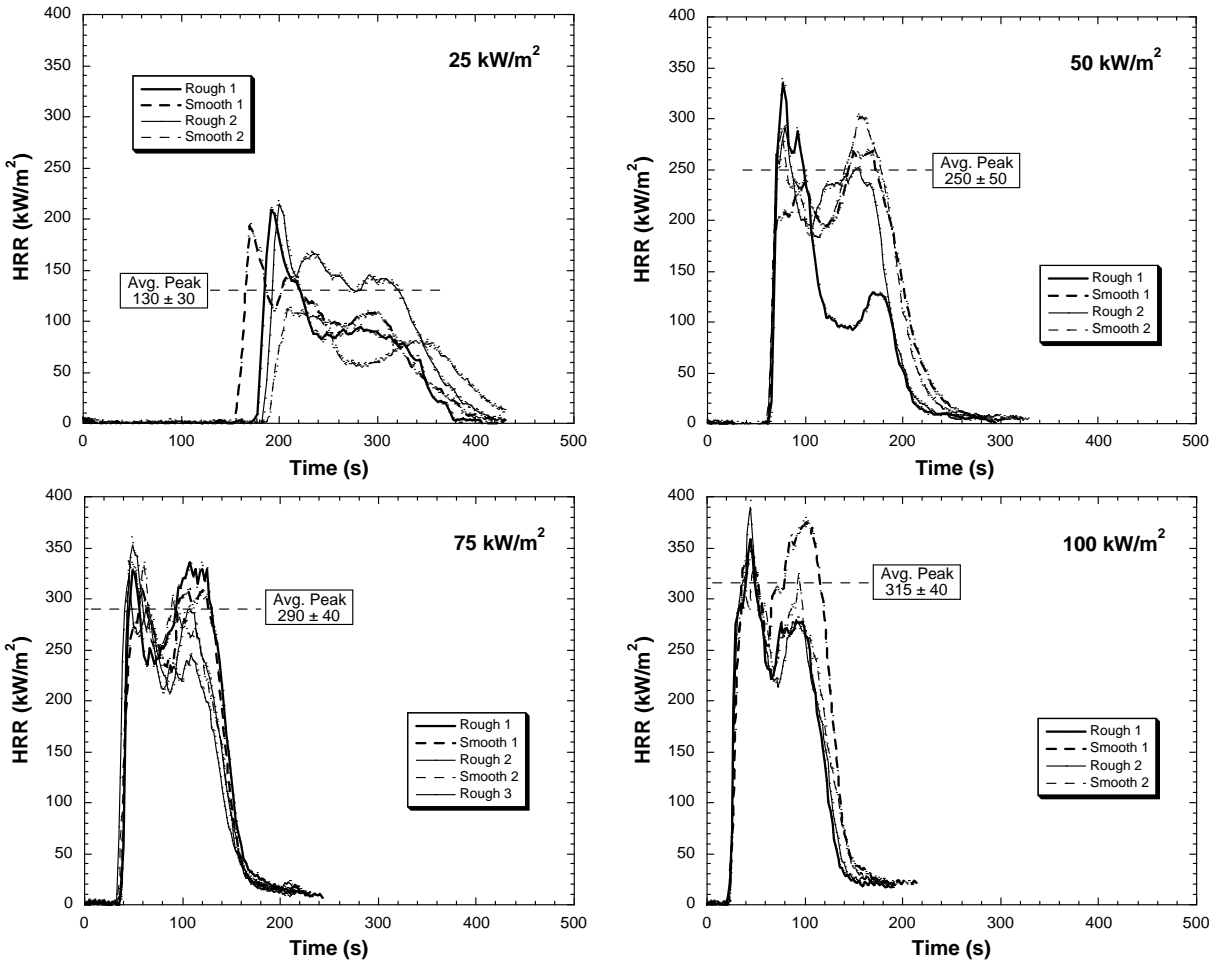


Figure 12. Heat Release Rate per Unit Area at Fluxes From 25 to 100 kW/m^2

An average peak HRR was estimated for each run shown in figure 12. Similar peak averages were obtained for runs below the critical heat flux for ignition. That ensemble of average peak HRR results is shown in figure 13. The burning rate was sustained for heat fluxes as low as 8 kW/m². According to theory, the critical HRR for sustained burning is about 50 kW/m² [3 and 4], which corresponds well to 8 kW/m² as about the critical heat flux for burning, CHF_b. The HRR provides enough heat to re-radiate back to the sample surface and sustain burning. The slope of the linear fit to the data gives the heat release parameter (HRP) as 2.87 [5]. The average heat of combustion (Δh_c) for the evolved resin vapors is 20 \pm 3 kJ/g-vapor, as shown in figure 14. The heat of gasification (L) can be determined since

$$\text{HRP} \equiv \Delta h_c / L \quad (10)$$

where $L = 7.0 \pm 1$ kJ/g-vapor. The heat of gasification is defined as the total energy absorbed by the sample per unit mass of volatiles under steady burning. Here, the burning is not steady in figure 12, but is at peak burning. At peak burning, the temperature in the sample is not expected to greatly change in time, and hence, the slope of the peak data can adequately yield the heat of gasification. It is defined for steady burning as the sum of the sensible heating (c_p term) and the heat of decomposition. The heat of gasification per unit mass of original material can be estimated accordingly as

$$h_g = (1 - \mu)L = (1 - 0.74)(7) = 1.8 \pm 0.3 \text{ kJ / g, original.} \quad (11)$$

This compares with the data from the DSC experiments as

$$h_g = \int_{T_\infty}^{T_{decomp}} c_p dT + \Delta h_{decomp} = 0.35 + 2.5 = 2.85 \pm 0.5 \text{ kJ/g - original.} \quad (12)$$

The difference most likely is due to the average peak slope determination of L .

The combustion efficiency is given by

$$\chi = \Delta h_c / \Delta h_{c,complete} = 20 / 26.5 = 0.75. \quad (13)$$

This suggests that the yield of soot and carbon monoxide is relatively high for flaming combustion.

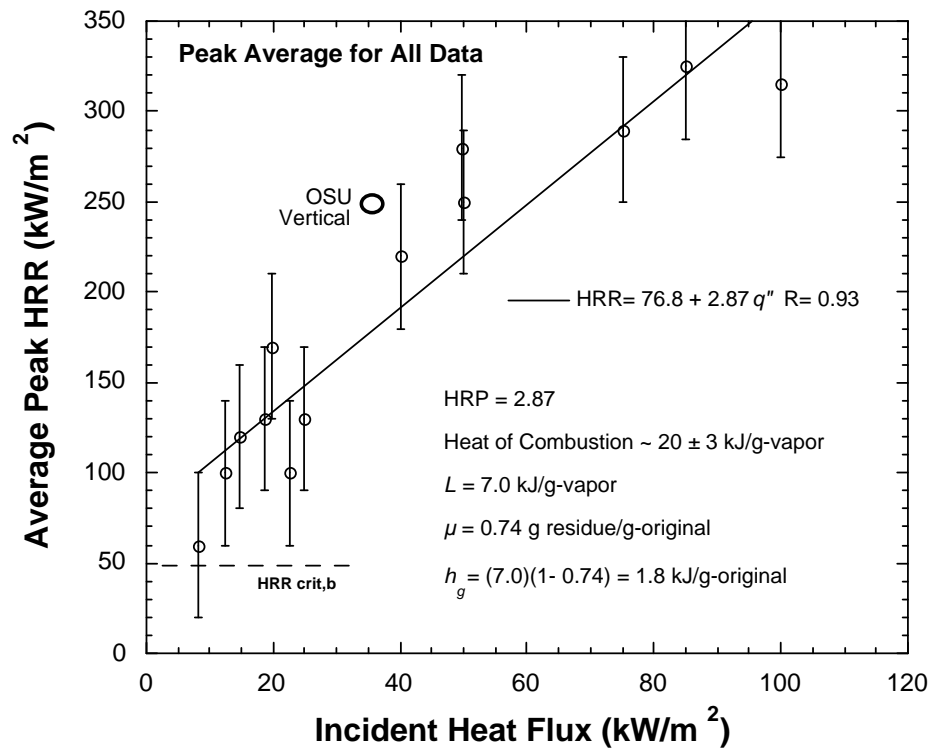


Figure 13. Average Peak HRR Over Burning Range

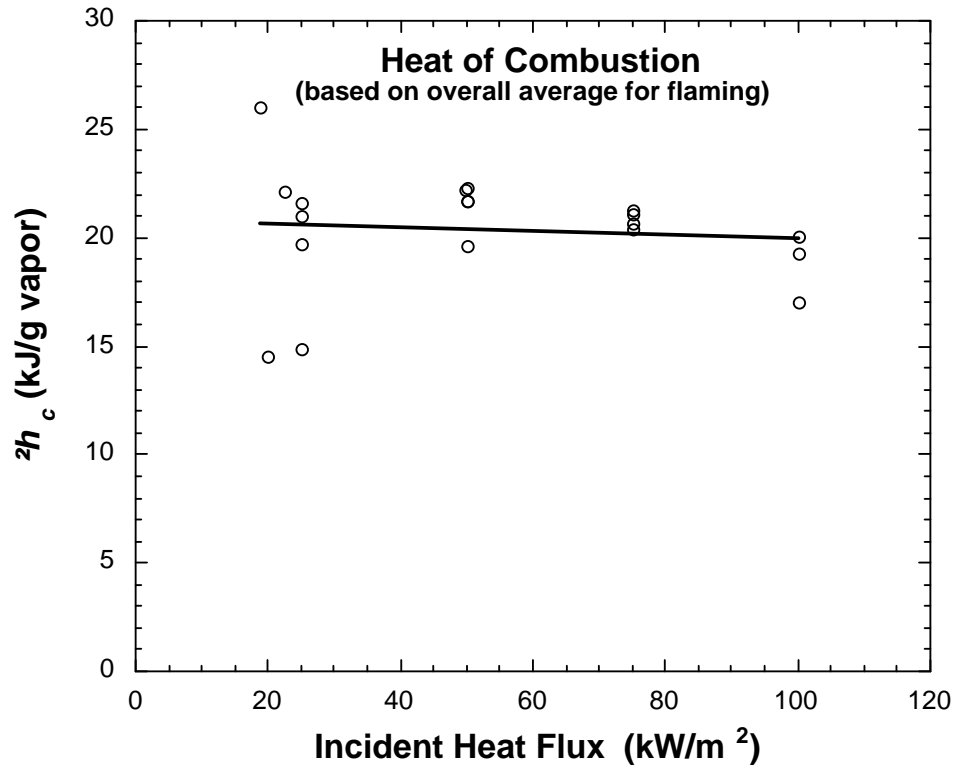


Figure 14. Heat of Combustion Over Range of Burning

It should be noted that the burning (caused by the ignitor) below the critical heat flux for ignition was not complete, and a significant portion of the resin did not burn at these lower heat fluxes, particularly when the igniter was removed. By subjecting the igniter alone to the cone calorimeter, its average HRR was recorded as about 120 kW/m². This is shown in figure 15, where the igniter was exposed alone during the 12.3 and 14.7 kW/m² runs. The net average peak HRR were estimated accordingly and are shown in the boxed labels of figure 12.

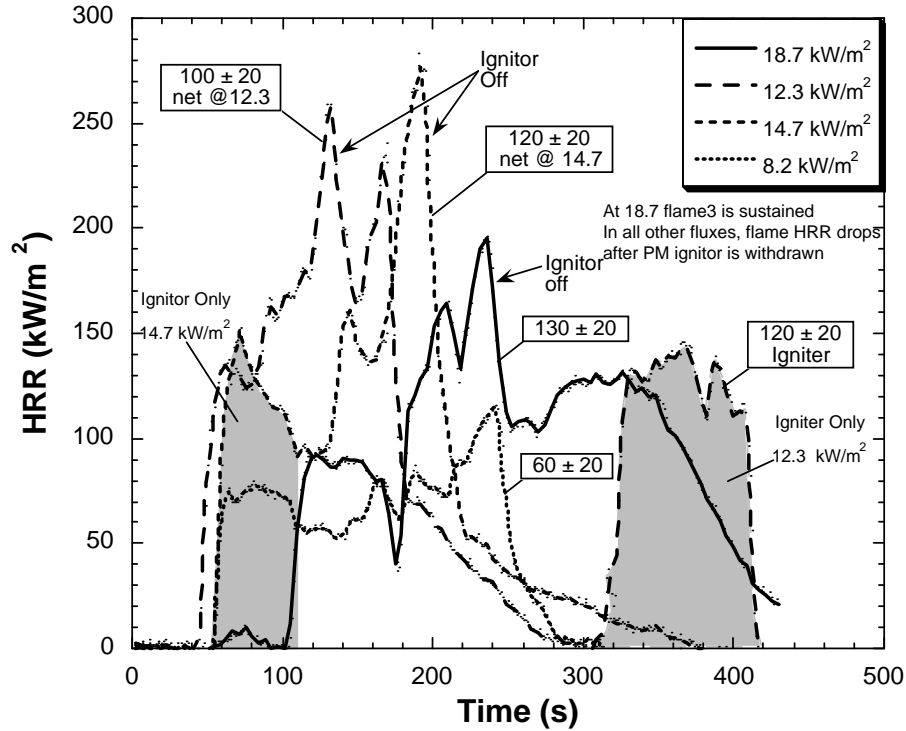


Figure 15. The HRR During the Critical Burning Series With Igniter

Figure 16 shows the THR per unit area during flaming. It clearly shows that at these lower heat fluxes, not all of the resin is burned. The THR is 30 MJ/m² for heat fluxes above 25 kW/m², but drops off linearly at lower values, falling to about 2 MJ/m² at 8 kW/m². While the initial flame and radiant heat fluxes can allow the burning to commence at the lower heat fluxes, as the resin is depleted, the carbon fibers insulate to reduce the internal heat flux. This causes extinction before all of the resin is consumed.

The carbon fibers will continue to oxidize following extinction of the flame due to the resin's combustion. This process was not fully explored to delineate its properties, but some features were established. The mass loss, after the flame extinguished, was examined for a limited period in the standard cone tests. In addition, at 85 kW/m², a thin blue flame about 2-3 mm off the surface persisted until the radiant heat flux was turned off. The burning rate for these cases is shown in figure 17.

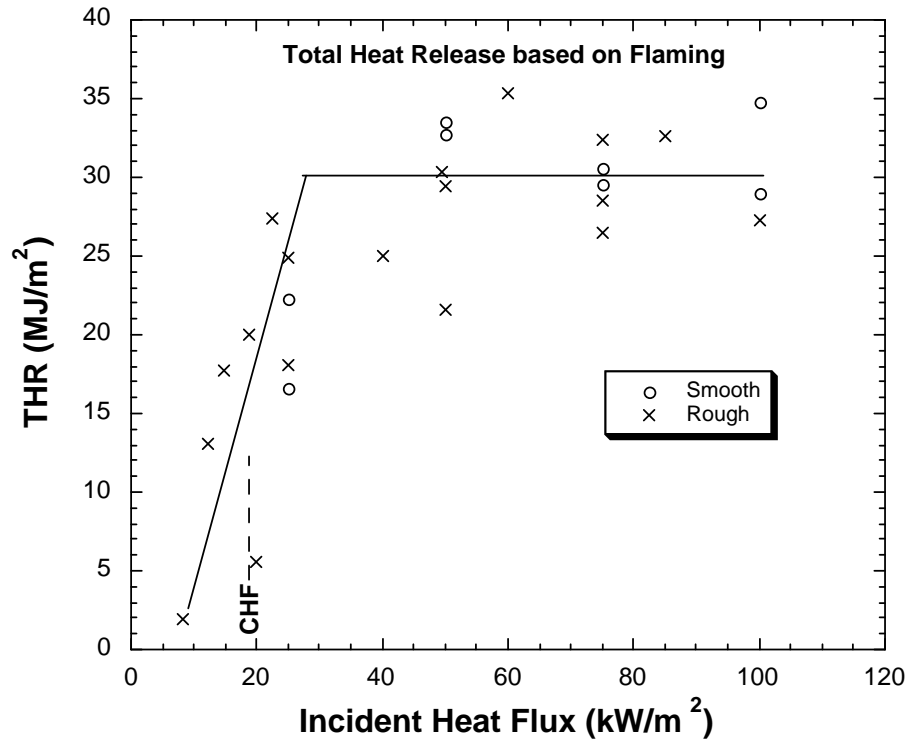


Figure 16. Total Energy Released in Burning

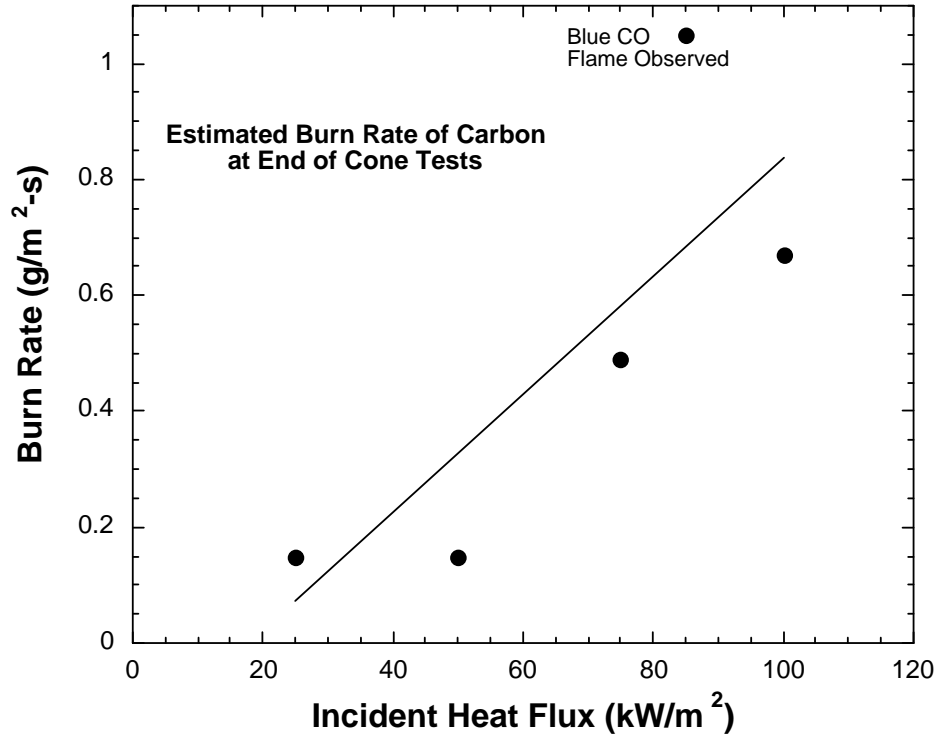


Figure 17. Burning Rate of Carbon Fibers in Smoldering

At sufficiently high temperatures, the smoldering oxidation of carbon will be sustained. The energy supply to the surface comes from the incident radiant heating and the energy produced in oxidation. At low temperatures (less than 500°C), the oxidation process is primarily controlled by kinetics, but at higher temperatures, the process of smoldering is controlled by the rate of oxygen transport to the surface. This transport depends on the convective field and, therefore, increases as the velocity of the stream increases. The carbon combustion rate at high temperatures is directly proportional to the heat transfer convective coefficient [9]. In the cone test, the heat transfer coefficient is roughly 10 W/m²-K [3]; under flight conditions this can be as high as 300 W/m²-K. Under natural convection conditions, the 3.2 mm composite sample tested would oxidize all of the carbon in about 1 hour at 85 kW/m². Under flight conditions, this could occur in about 2 minutes provided the heat flux can be sustained.

Surface temperatures of the composite were measured in several tests following flaming combustion. These temperatures constitute the condition of surface smoldering. The values are plotted in figure 18 along with the blackbody temperature corresponding to the incident heat flux. It shows that the convective and conduction losses from the surface exceed the energy released in smoldering. The smoldering energy is of the order of 5-35 kW/m².

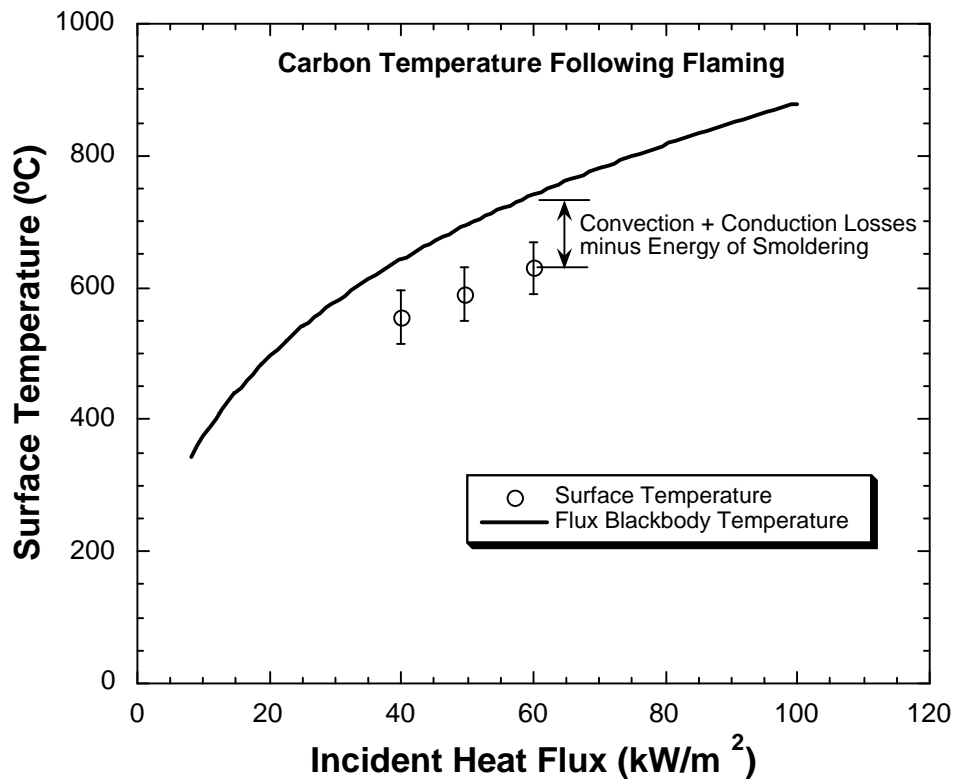


Figure 18. Surface Temperatures of Carbon Fiber Smoldering

2.6 YIELDS AND MORPHOLOGY OF BURNING.

The composite material decomposes and burns under heating by vaporizing the resin binding the carbon fiber plies. As the resin vaporizes, it seeks to escape through the fibers, and this process develops pressure in the composite. Those stresses result in a volume increase for the remaining matrix of material. Under flaming, that pressure can cause jets to emerge that distort the normal natural convection flame on the surface. This is particularly evident in the burning of a vertical sample, as done in the OSU apparatus. A photograph of the enlarged boundary layer flame due to jetting is shown in figure 19. After flaming, the composite generally is depleted of the resin if combustion is complete, and this was shown to be the case for heat fluxes above about 25 kW/m^2 according to figure 16. However, char from the resin can remain, and this is roughly 0.25 as a char mass fraction based on the resin alone [10]. As the resin and its char are depleted, the carbon plies can lose their structural integrity. It was observed that for the case of 85 kW/m^2 , in which the sample was allowed to smolder for some time after flaming ceased, the fiber structure lost its rigid composition upon handling. The composition became more loosely hair-like with increasing handling. Photographs of the final state of the composite after burning are shown in figure 20a through 20h. The aluminum foil in the photographs was either due to wrapping the back for the cone test, or due to sealing in volume determination tests (blue in some photographs).



Figure 19. Vertical Burning in the OSU Apparatus



Figure 20a. After Burning Front and Back, 8.2 kW/m^2

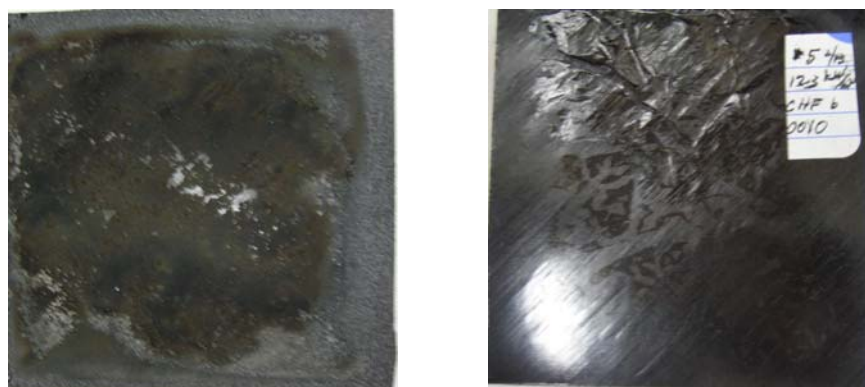


Figure 20b. After Burning Front and Back, 12.3 kW/m^2



Figure 20c. After Burning Front and Back, 14.7 kW/m^2



Figure 20d. After Heating Front and Back, 17.5 kW/m²



Figure 20e. After Burning Front and Back, 18.7 kW/m²

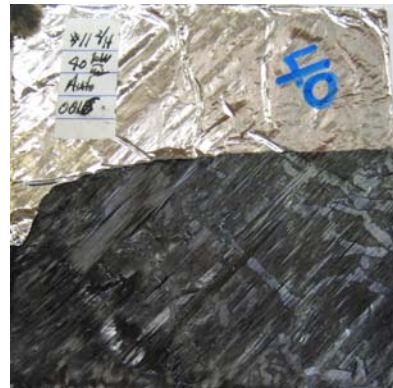
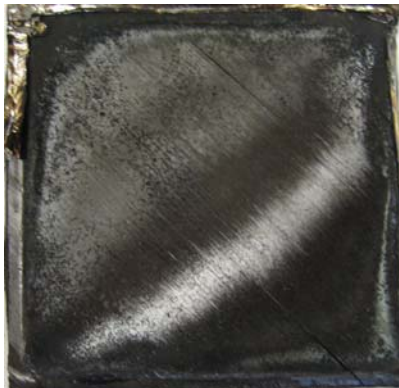


Figure 20f. After Burning Front and Back, 40.0 kW/m²

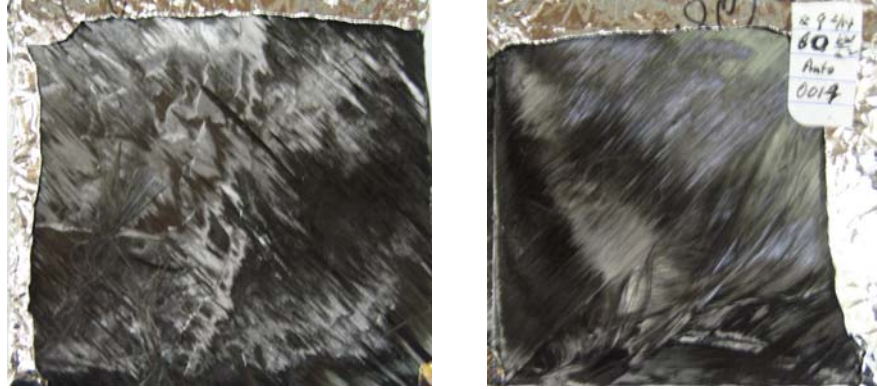


Figure 20g. After Burning Front and Back, 60.0 kW/m²



Figure 20h. After Burning Front and Back, 85 kW/m²

Figure 21 displays the typical swelling of the composite on heating. As the edges are constrained in the cone holder, the swelling is mostly at the center. The thickness increase at the center was measured, and an attempt was made to measure the volume increase. The volume was measured by immersing the sample in a beaker of water and measuring the volume displaced.



(a) At 40 kW/m²



(b) Original

Figure 21. Thickness Increase on Burning

For the more degraded samples, an increase in mass of the sample indicated the absorption of water. By weight measurements before and after immersion, the true displaced volume of the outer envelope of the sample could be estimated. The initial volume was 32 cm³, and thickness was 3.2 mm. Figure 22 shows the increases in volume and thickness. In addition, the porosity (P) of the expanded sample (void volume to final volume) and the mass fraction (μ_{char}) of the resin remaining as char or undepleted resin were estimated. These follow from

$$P = 1 - \left[\phi_{c,i} + \frac{\rho_R}{\rho_{char}} (1 - \phi_{c,i}) \mu_{char} \right] \quad (14)$$

and

$$\mu_{char} = \frac{\rho_i (m_f / m_i - \mu_{c,i})}{\rho_R (1 - \phi_{c,i})} \quad (15)$$

where

- the initial bulk density, $\rho_i = 1.54 \text{ g/cm}^3$
- the initial carbon fiber mass fraction, $\mu_{c,i} = 0.68$
- the initial carbon fiber volume fraction, $\phi_{c,i} = 0.60$
- the resin density, $\rho_R = 1.22 \text{ g/cm}^3$
- the char density, $\rho_{char} = 1.75 \text{ g/cm}^3$ (as an estimate)

For heat fluxes above about 25 kW/m², complete burning of the resin takes place and the properties associated with expansion appear to approach an asymptote. The maximum volume expansion factor is about 2.2, the porosity is about 0.65, and the char fraction of the resin appears to approach its nominal value of about 0.25.

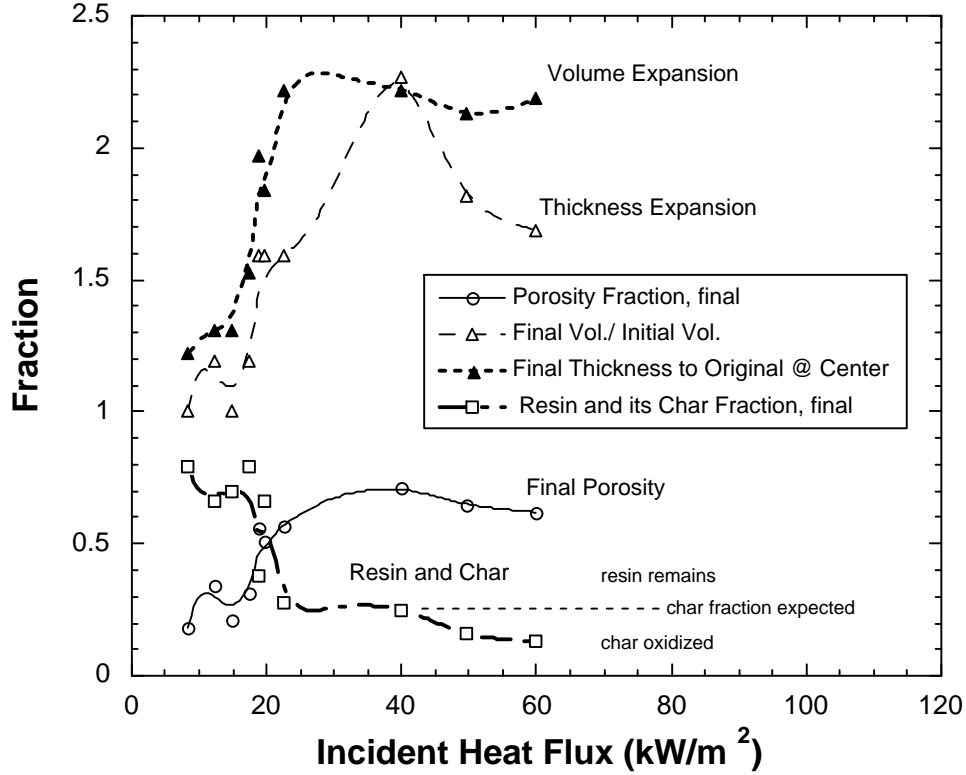


Figure 22. Morphology of Composite After Burning

It should be noted that in a full transport model of the degrading composite, Darcy's Law would have to be employed to measure the mass flux of the flowing vapors as a function of pressure gradient. The coefficient of proportionality in this transport process is the ratio of the permeability to the kinematic viscosity. The permeability is related to the porosity, but specifically depends on the effective diameter (squared) of the pores along the flow path. As the void volume plus the initial carbon fiber volume compose the final volume in complete burning of the resin, a uniform distribution of fibers distributed monodirectionally yields an effective pore void diameter (d) in terms of the fiber diameter ($d_c = 7 \mu\text{m}$).

$$d = \left(\frac{P}{1-P} \right) d_c \quad (16)$$

This gives an effective pore diameter of $8.5 \mu\text{m}$. A cut cross section of the 40 kW/m^2 burned sample, displayed in figure 20f and 21(a), is shown in figure 23. The expansion appears to have occurred uniformly over the plies and confirms the estimate of the pore diameter given here.



Figure 23. Cross Section of the 40 kW/m² Heated Composite

2.7 YIELDS OF INCOMPLETE COMBUSTION PRODUCTS.

The primary incomplete products of combustion for the flaming resin are CO and soot. The cone calorimeter data includes concentration measurements of CO and light obscuration of the smoke. Tewarson [11] best explains how these measurements are converted into yields based on per unit mass of vapor burned. The heat of combustion given in figure 13 is the yield of chemical energy released per unit mass of vapor. Similarly, the yield of CO and smoke are computed and averaged over the flaming period. They all serve to give the average stoichiometry of the combustion reaction of the vapor with air.

Figure 24 gives the yield of CO for flaming conditions. As with the heat of combustion of figure 14, the yield reaches an asymptote (~ 0.048) for complete burning of the resin after about 25 kW/m². Note, under smoldering conditions, nearly all of the carbon will yield CO, but it could be burning completely to CO₂ if a flame forms near the surface, as discussed for the sample burned at 85 kW/m².

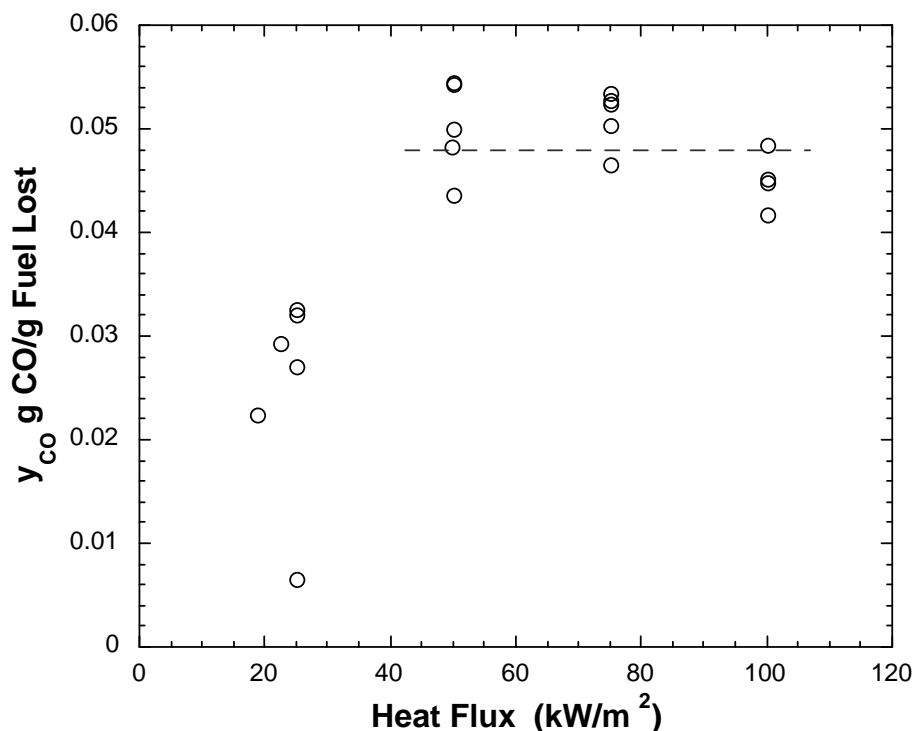


Figure 24. Yield of CO for Flaming Conditions

The parameter measured for smoke is the mass optical density (D_m), and it expresses the visibility per unit mass of fuel lost. It is directly related to the yield of soot or particulates in the smoke. It also relates to the specific optical density (D_s) quantity measured in the National Bureau of Standards smoke density chamber (SDC) as

$$D_s = D_m (\Delta m_{lost} / A) \quad (17)$$

where $\Delta m_{lost}/A$ is the mass lost per unit surface area of heated specimen. As D_s is a dimensionless quantity inversely related to the transmission of light (i.e. $I/I_o \sim \exp(-D_s)$), the attenuation by the smoke increases as $\Delta m_{lost}/A$ increases. The mass optical density approaches a constant of roughly $850 \text{ m}^2/\text{kg}$ of mass lost as shown in figure 25.

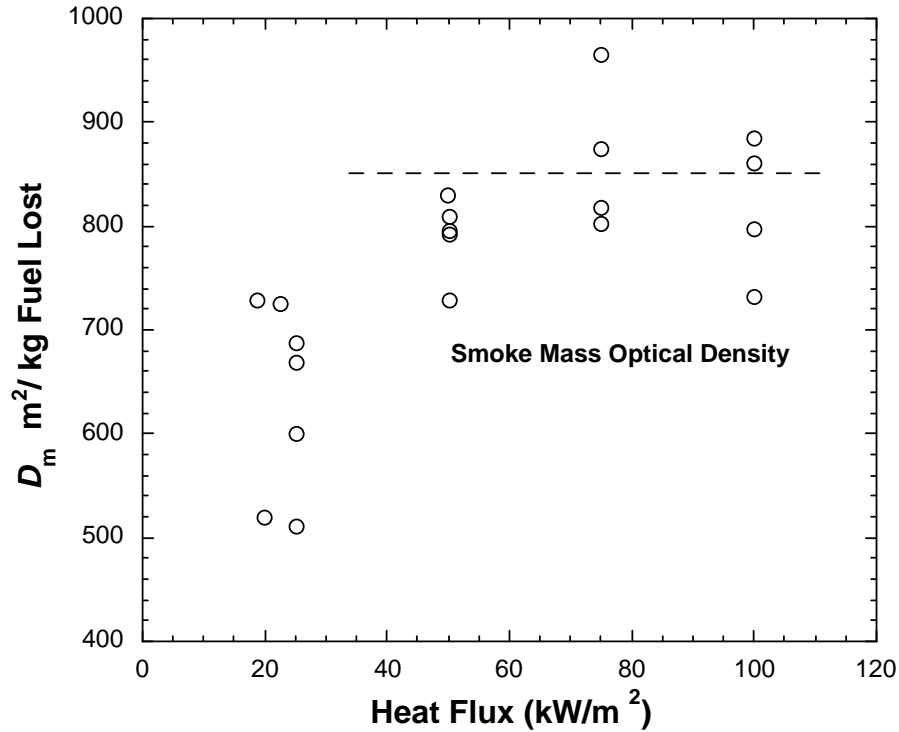


Figure 25. Yield of Smoke for Flaming Conditions

The smoke density of the composite measured in the smoke density chamber gave results as shown in figure 26. Here a vertical sample is irradiated at 25 kW/m^2 and small premixed flames near the bottom promote piloted ignition. The results of the standard test for the composite is shown in figure 26 along with a prediction using equation 17 based on the mass loss rate in the cone at 25 kW/m^2 . The difference between the standard result and the prediction is due to the transient burning behavior between the standard vertical configuration and the horizontal sample orientation in the cone. This result also shows the limitation of addressing smoke hazard by the standard test, as the smoke visibility for the composite is clearly a function of ignition time and the early rate of burning. The hazard of smoke visibility needs to address the nature of the fire scenario. The SDC is a closed system at the start of burning and pertains to the volume of that chamber and the area of burning.

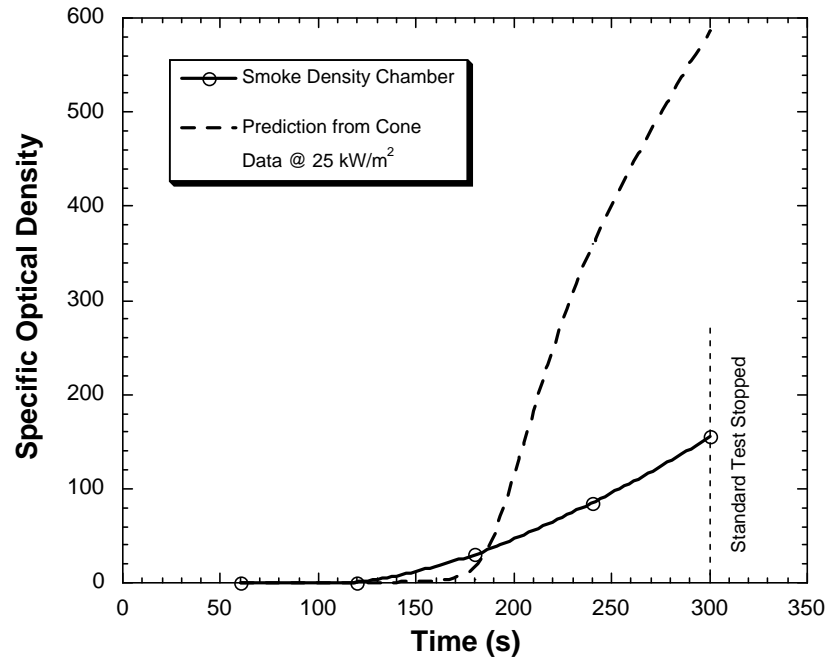


Figure 26. The D_s for the Smoke Density Chamber

The fractional residue of carbon fibers and resin char that remains after flaming was suggested by TGA data to be 0.74. The results in the array of cone tests are shown in figure 27 to vary with heat flux, which is consistent with the TGA result.

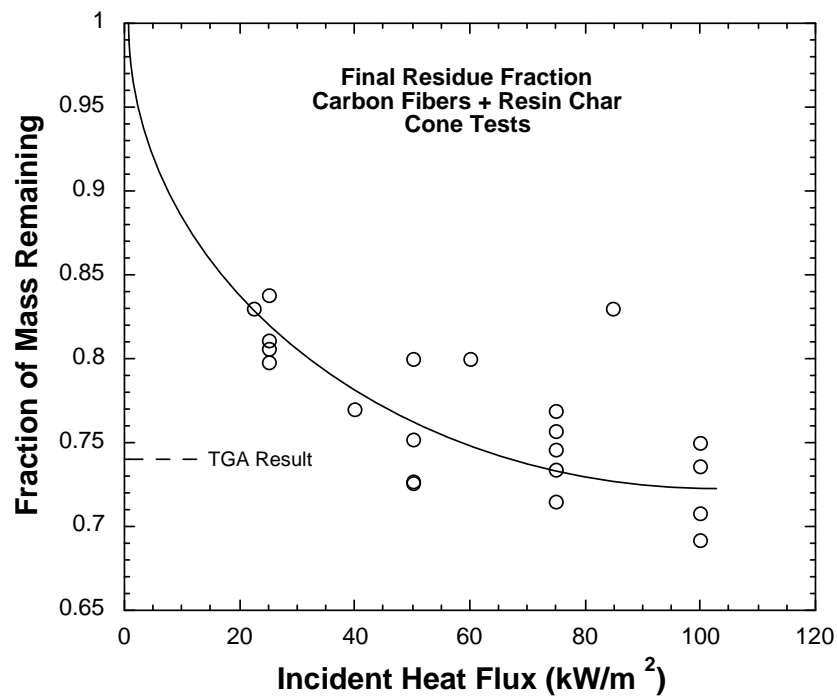


Figure 27. Residue Fraction After Flaming

2.8 FLAME SPREAD.

A special radiant panel apparatus was used to investigate the conditions of flame spread for the composite. The apparatus was developed in the work of Panagiotou and Quintiere [12], and is depicted in figure 28. The composite was tested in an exposed dimension of approximately 6 by 25 cm long. The sample had to be specially prepared by applying an adhesive ceramic coating to the edges to prevent out-gassing along the edges. Only surface flames must appear in a proper test to reflect no exposure size factors. The tests were run with preheating at the designated heat flux to establish a steady temperature on the surface. The preheating time was set at 4 minutes, corresponding to the time to reach the critical heat flux as derived from the curve shown in figure 8 (i.e., $0.065^{-2}/60 = 3.9$ min.). The flame spread is only a unique function of heat flux at this long-time condition, as the flame speed depends on surface temperature. A video camera behind the radiant panels recorded the flame spread as shown in figure 29. A reduction of these data allowed an estimate of the flame tip and the pyrolysis position. If the speed of the pyrolysis front is steady, the speed of the flame tip will be identical. A typical reduction of the video data is shown in figure 30. By comparing the time to ignite with the ignition data (figure 8), the 6-cm-tall igniter flame is estimated to have had a net flame heat flux of about 60 kW/m^2 . The flame tip velocity was slightly higher than the pyrolysis front speed, but the flame speed did appear constant for about 100 s. After that time, the flame speed decreased, and its advancement stopped. The igniter was sustained over the entire time.

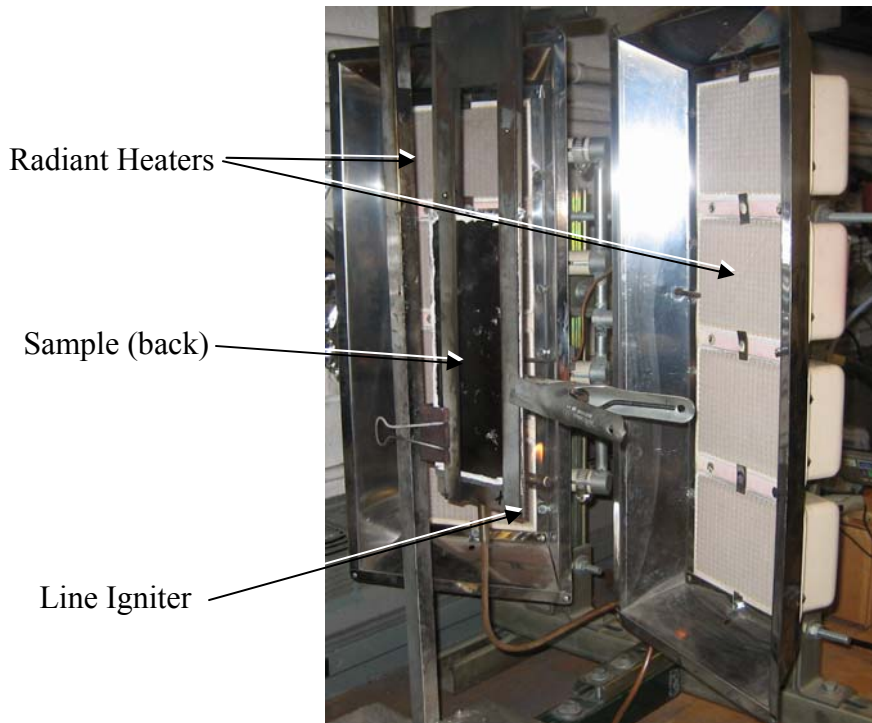


Figure 28. Flame Spread Apparatus



Figure 29. Vertical Flame Spread

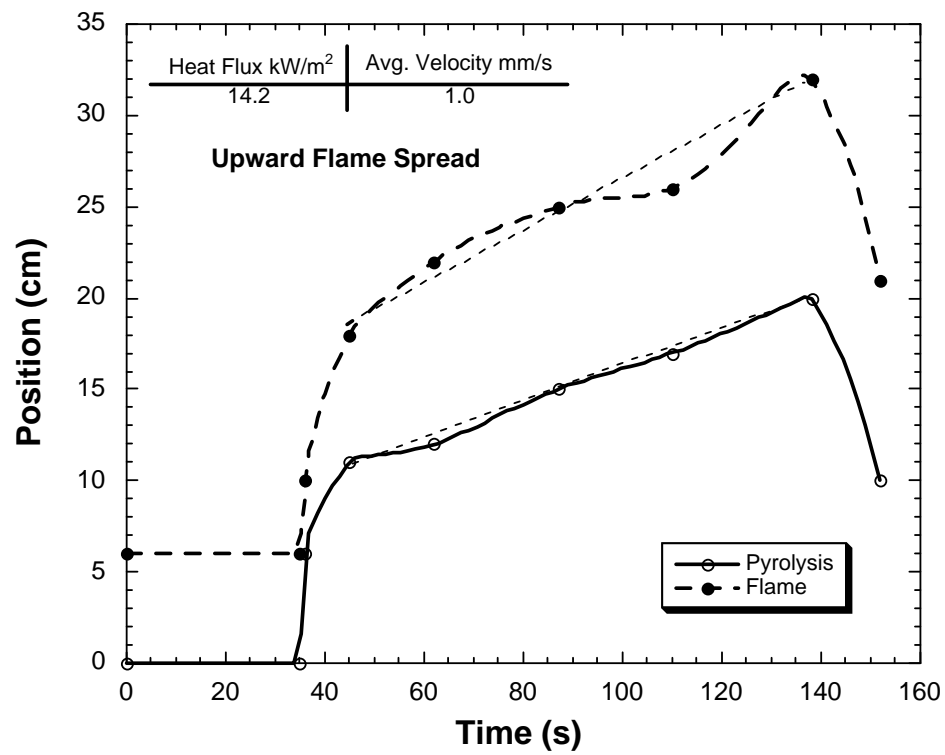


Figure 30. Pyrolysis and Flame Tip in Vertical Spread

All vertical flame spread data exhibited this decay in speed after some time. It would appear that the igniter flame had some influence, but more likely the decrease in the burning rate of the composite caused the decrease. The flame spread was investigated in a horizontal orientation and vertically downward. The heat flux available was not able to spread the flame initially. All flame spread results determined in this study are shown in figure 31. At the critical flux for piloted ignition, the flame spread would approach the premixed speed (~ 50 cm/s) as the surface temperature would approach the ignition temperature. The critical heat flux for upward flame spread is < 10 kW/m², for downward is between 14 and 18 kW/m², and for horizontal is between 6 and 18 kW/m². The limitations of the apparatus on achieving sufficient heat fluxes for spread on downward and horizontal orientations prohibited more precise results. The nature of the upward spread observed is shown in figure 32.

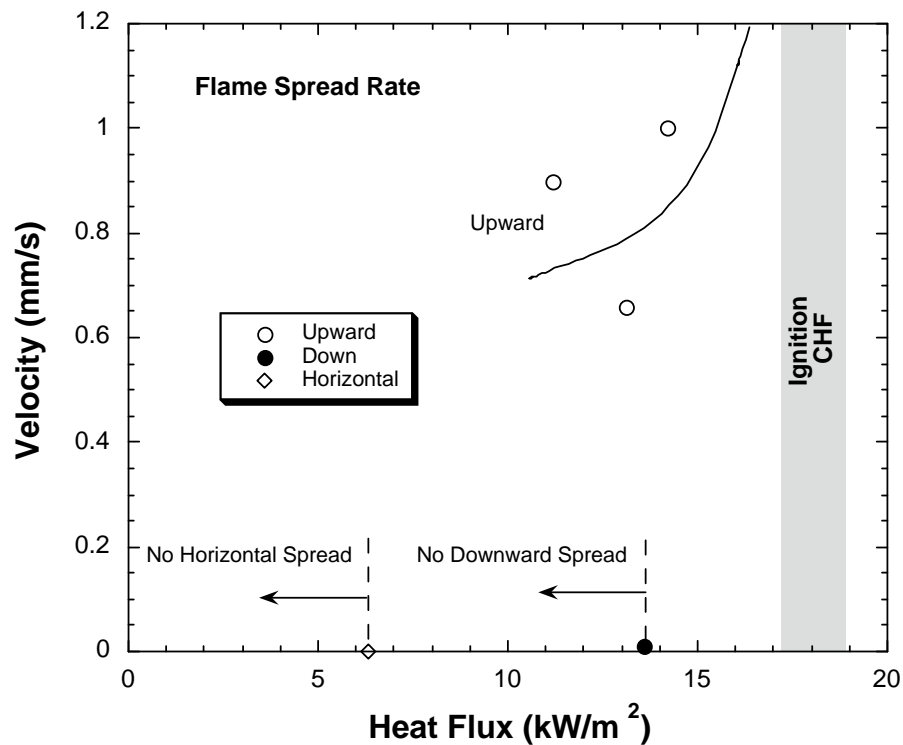


Figure 31. Flame Speed Dependence on Heat Flux

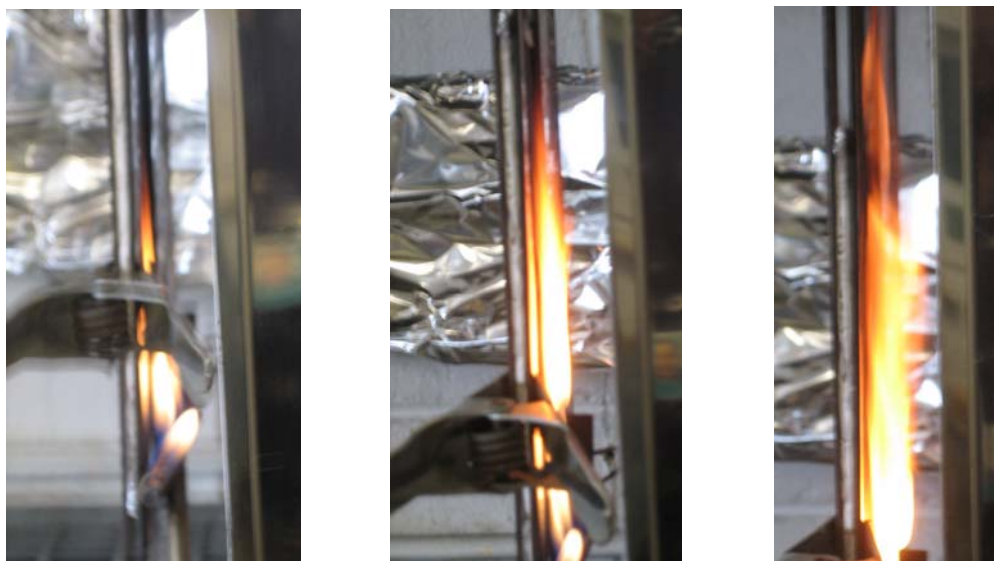


Figure 32. Upward Flame Spread Behavior

3. SUMMARY OF RESULTS.

The data presented herein constitute a set of information useful for characterizing the burning behavior of the Toray Composites BMS 8-276 carbon-fiber material. A summary of the results is presented in table 2. The parameters constitute the properties related to thermal heating, degradation, burning, and the physical morphology of the material undergoing thermal degradation. All results were conducted in air, except for the microcalorimeter and TGA/DSC where degradation was performed in nitrogen. The effect of increased oxygen will have minimal effect on the piloted ignition temperature, reduce the auto-ignition temperature, linearly increase the burning rate, and cause the flame spread rate to increase at most with the square of oxygen concentration [3]. The effect of increased thickness would be to increase burning time and somewhat delay ignition times for heat fluxes below about 43 kW/m^2 . Complete vaporization of the resin occurred for heat fluxes above 25 kW/m^2 in the cone calorimeter with an insulated backface. Under these conditions, the heat of combustion was approximately 20 kJ/g-vapor , the yield of CO in flaming was roughly $0.48 \text{ g CO/g-vapor}$, and the mass fraction of remaining residue was roughly 0.74. The sample can swell to over twice its volume, and its porosity after burning is about 65%. The minimum heat flux required for auto-ignition is 32 kW/m^2 , for piloted is 18 kW/m^2 , and for burning is about 10 kW/m^2 . Flame spread will occur for heat fluxes below 18 kW/m^2 after preheating for 4 minutes with upward flame spread occurring for as low as 10 kW/m^2 with rates of the order of 1 mm/s .

Table 2. Summary of Toray Carbon-Fiber Composite

Property	Value	Comments
Thickness	3.2 mm	
Density	1530 kg/m ³	
Thermal conductivity at 25°C at 300°C	0.13 W/m-K 0.32 W/m-K	Heat loss error could result in about 20% lower values
Specific heat at 25°C at 300°C	0.85 J/g-K 1.98 J/g-K	
Decomposition temperature • Onset • Range	300°C 650°C, max	Significant range is 400° - 500°C
Heat of decomposition	2.5 kJ/g original	
Activation energy to pyrolysis	182 kJ/mol	First-order reaction fit
Pre-exponential coefficient	$9.67 \times 10^{10} \text{ s}^{-1}$	
Heat of combustion • Complete • Actual	26. 5 kJ/g vapor 20 ±3 kJ/g vapor	From microcalorimeter From cone
Effective heat of gasification	7 ±1 kJ/g vapor 1.8 ±0.3 kJ/g- original 2.85 ±0.5 kJ/g- original	Based on average peak From cone data From DSC
Critical heat flux • Auto ignition • Piloted ignition • Burning • Upward flame spread • Downward flame spread • Horizontal flame spread	32.0 kW/m ² 18.0 kW/m ² ~ 8.0 kW/m ² ~ 10 kW/m ² 14 to 18 kW/m ² 6 to 18 kW/m ²	Combustion not complete Flame dies out
Total heat release per thickness	9.4 MJ/m ² -mm	> 25 kW/m ²
CO yield in flaming	0.48 ±0.05 g/g vapor	> 25 kW/m ²
Smoke mass optical density	0.85 ±0.05 g/g vapor	> 25 kW/m ²
Residue fraction after flaming	0.74	Carbon fibers + resin char
Porosity after flaming	0.65 ±0.05	> 25 kW/m ²
Volume expansion	2.2 ±0.1	> 25 kW/m ²
Char yield from resin	0.20 ±0.05	> 25 kW/m ²

4. CONCLUSIONS.

This report has presented the properties of a carbon composite typical of aircraft construction. The resin binding the carbon fibers comprises about 30% of its mass and will burn with a char residue of about 20%. The properties of the composite under fire heating conditions and burning have been measured and can be used in modeling and explaining attributes of fire performance of this material. It should be realized that the properties pertain primarily to the characteristics of the resin material, as the carbon fibers do not generally burn. Also, the burning tests are peculiar to horizontal burning in the cone calorimeter and, therefore, depend on the flame heat flux generated in that test and the insulated nature of its back face. Otherwise, the results are expected to be general, and not test dependent.

5. REFERENCES.

1. Stoliarov, S.I., Walters, R.N., and Lyon, R.E., "Determination of Heats of Gasification of Polymers Using Differential Scanning Calorimetry," *Proc. 52nd Intl. SAMPE Symposium & Exhibition*, Baltimore, MD, June 4-6, 2007.
2. Lyon, R.E. and Walters, R.N., "Microscale Combustion Calorimeter," US5981290, November 09, 1999.
3. Kim, M. and Quintiere, J.G., "Predicting Polymer Burning Using TGA/DSC," *5th Int. Seminar on Fire and Explosion Hazards*, Edinburgh, 23-27 April 2007.
4. Lyon, R.E., "Piloted Ignition of Combustible Solids," *Fire and Materials, 9th International Conference*, San Francisco, CA, January 31, 2005.
5. Quintiere, J.G., "A Theoretical Basis for Flammability Properties," *Fire and Materials*, March 29, 2006.
6. Spearpoint, M.J. and Quintiere, J.G. "Predicting the Piloted Ignition of Wood in the Cone Calorimeter Using an Integral Model - Effect of Species, Grain Orientation and Heat Flux," *Fire Safety Journal*, 36, 2001.
7. FAR 25.853 a-1, "Heat Release Test for Cabin Materials," compiled by April Hornor, Aircraft Materials Fire Test Handbook, FAA report DOT/FAA/AR-00/12, April 2000.
8. ASTM E 1354, "Standard Test Method for Heat and Visible Smoke Release Rates for Materials Using an Oxygen Consumption Calorimeter," American Society of Testing and Materials, Philadelphia, PA, 1992.
9. Glassman, I., *Combustion*, Academic Press, NY, 1977.
10. Lyon, R.E., FAA William J. Hughes Technical Center, Private Communications, May 2007.

11. Tewarson, A., "Generation of Heat and Chemical Compounds in Fires," Sec. 3, Chap. 4, *The SFPE Handbook of Fire Protection Engineering*, 3rd ed., pp. 3-82 to 3-161, The National Fire Protection Association Press, Quincy, MA, 2002.
12. Panagioutou, J. and Quintiere, J. G., "Generalizing Flammability of Materials," *Interflam 2004*, Edinburgh, July 2004.